Journal of Industrial and Management Optimization

https://www.aimspress.com/journal/jimo

JIMO, 22(1): 450–485.
DOI:10.3934/jimo.2026017
Received: 21 August 2025
Revised: 02 November 2025
Accepted: 20 November 2025
Published: 15 December 2025

Research article

Power control of generator sets in coal-fired power plants based on the combination of MPC and neural network PID

Minan Tang* **, Shengqi Zhang , Zhongcheng Bai and Chuntao Rao**

College of Automation and Electrical Engineering, Lanzhou Jiaotong University, Lanzhou 730070, China

* **Correspondence:** Email: tangminan@mail.lzjtu.cn; Tel: +86-138-9368-8178.

Abstract: Reliable generator power control is vital for the stability of coal-fired power plants. This study proposes a strategy that integrates model predictive control (MPC) with a neural network PID controller to address the nonlinear and complex dynamics of generator systems. The boiler–turbine–generator (BTG) unit is modeled as a representative three-input, three-output nonlinear system. To mitigate excessive overshoot in traditional PID controllers, a BP neural network adaptively adjusts PID parameters, enabling real-time learning of system dynamics and improving transient response. Furthermore, MPC is combined with the BP neural network PID controller, where rolling horizon prediction and feedback correction ensure precise power regulation, reduced steady-state error, and enhanced dynamic performance. A 660 MW generator model is established in MATLAB/Simulink, and the proposed approach is compared with traditional PID and BP neural network PID control. Simulation results confirm the superiority of the proposed approach. It nearly eliminates overshoot, reducing it to 3.0% from 43.9% (traditional PID) and 24.2% (BP NN-PID control). Unlike the slower BP-NN PID, our method maintains a rapid 450-second settling time, comparable to the traditional PID. This combined improvement in stability and speed results in the integral absolute error (IAE) being reduced by 85% and approximately 77% compared to the traditional PID and BP neural network PID controllers, respectively.

Keywords: thermal power generation; power control; neural network PID; model predictive control; generator set
Mathematics Subject Classification: 93C40, 93B52; Secondary: 68T07, 93C95

1. Introduction

Driven by global efforts to combat climate change and to achieve the strategic goals of "dual carbon" (carbon peaking and carbon neutrality), renewable energy sources such as wind power and

photovoltaics are being integrated into modern power systems at an unprecedented rate [1, 2]. However, the inherent intermittency and high volatility of new energy sources pose serious challenges to the frequency stability and power quality of the power system [3]. Against this backdrop, traditional coal-fired power generation units, regarded as the "ballast" and "stabilizer" of the current power system, are experiencing a profound transformation in their functional role. They are not only expected to continue ensuring reliable baseload power supply but are also entrusted with the critical mission of providing flexible regulation capabilities, including deep peak shaving and rapid response, to accommodate the large-scale integration of renewable energy [4, 5]. Therefore, how to improve the power control performance of coal-fired units through advanced control technology, i.e., enhancing their response speed, regulation accuracy, and operational stability, has become one of the core technical bottlenecks in ensuring the safe and economical operation of future high-proportion renewable energy power systems [6, 7]. This study addresses this issue by proposing a neural network PID control strategy optimized through model predictive control (MPC). The objective is to enhance the power control performance of coal-fired power plant generators and to provide an advanced control solution to support the development of next-generation power systems.

Coal-fired power plants still play a dominant role in the power generation mix and serve as critical infrastructure for ensuring national energy security and a stable electricity supply [8]. A thermal power plant is a complex thermal system. Its fundamental principle is to use coal combustion to heat water in a boiler, generating high-temperature, high-pressure steam to drive a turbine, which in turn drives a generator to produce electricity. After performing work, the steam is condensed into water in a condenser and then recycled back to the boiler for reuse [9]. In this process, precisely coordinating the dynamic responses of the boiler and turbine to achieve stable power control of the generation unit directly impacts the frequency stability and operational efficiency of the entire power grid, which carries significant practical importance [10]. Therefore, in-depth research and optimization of this core link is key to improving the efficiency and stability of the entire energy system. The workflow of a coal-fired power plant is shown in Figure 1.

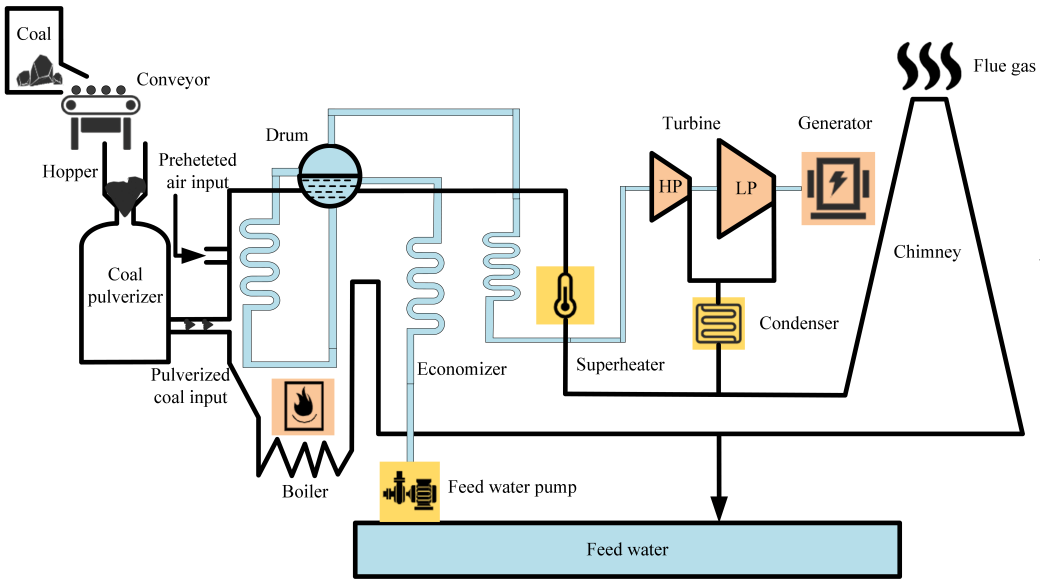

Figure 1. Workflow diagram of a coal-fired power plant.

Coal-fired power generation units, being complex and nonlinear control objects, have been the subject of extensive and in-depth research by scholars worldwide in the field of power control. Traditional PID controllers have dominated industrial applications over the past several decades due to their simple structure and robust performance. However, they exhibit limitations in dynamic response, steady-state accuracy, and disturbance rejection, making it challenging to meet the precise control requirements under varying operating conditions [11, 12]. To address the limitations of traditional PID control, researchers have proposed a variety of intelligent control strategies, including adaptive control [13, 14], fuzzy control [15–17], neural network control [18–20], and decoupling control [21–23], among other advanced approaches. Researchers have employed fuzzy logic control to emulate expert knowledge in order to address system uncertainties and nonlinearities, thereby improving control performance to some extent [24]. In addition, researchers have investigated the integration of PID control with intelligent algorithms, leading to the development of hybrid PID control approaches. Machine learning techniques, particularly neural networks, have been incorporated into controller design, enabling a deep integration of neural network architectures with numerical optimization methods. This approach has gradually emerged as an effective pathway for enhancing the response performance of nonlinear systems, as exemplified by studies on the stability analysis of recurrent neural networks and the exploration of non-convex optimization control based on neural networks [25, 26]. These controllers exhibit superior control performance in complex industrial process applications, including boiler temperature regulation, power load management, and liquid level control systems. In [27], researchers addressed the challenge of online optimization of traditional PID controller parameters by designing a real-time temperature control system integrated with neural networks. This approach leverages the self-learning capabilities of neural networks to achieve online adaptive tuning of PID parameters, thereby enhancing the system's control performance in dynamically changing environments. To address the limitations of traditional PID controllers in achieving satisfactory control performance for strongly nonlinear systems, a previous work [28] proposed an adaptive PID control strategy based on neural networks. This approach exploits the nonlinear modeling capabilities of neural networks to perform online adjustment of controller parameters, effectively enhancing the system's dynamic response and steady-state accuracy and demonstrating superior control performance across multiple nonlinear systems. Neural network PID controllers offer advantages such as self-learning, self-adaptation, and self-organization. They are capable of performing online parameter identification of the controlled system and automatically adjusting control parameters in response to changes in system states, thereby achieving superior control performance under complex operating conditions. By leveraging the self-learning and nonlinear mapping capabilities of neural networks, PID parameters can be dynamically optimized online, enhancing the controller's adaptability to system uncertainties and nonlinear characteristics. Nevertheless, achieving fully ideal control performance in complex systems remains a significant challenge [29–32]. In recent years, fractional-order PID (FOPID) controllers combined with advanced meta-heuristic and intelligent optimization algorithms have also attracted increasing attention in power system control. Authors in [33] proposed a fractional-order PID controller tuned by the Artificial Protozoa Optimizer (APO) for load frequency regulation (LFR) in multi-area interconnected power systems, achieving superior frequency stability and faster convergence compared with conventional PID methods. In [34] it was developed a neural network-based fractional-order PID algorithm for load-frequency control, demonstrating enhanced adaptability and dynamic performance

under parameter uncertainties. In addition, [35] a Slime Mold Optimizer (SMO) has been introduced to tune a cascaded PD–PI controller, significantly improving damping characteristics and reducing steady-state error in multi-area thermal power systems. These studies highlight the trend of combining fractional-order control structures with bio-inspired optimization algorithms to further improve frequency stability and control performance in large-scale power systems. However, most of these works mainly address load-frequency regulation in multi-area systems rather than the nonlinear power control of boiler–turbine–generator (BTG) units considered in this paper. Whether employing fuzzy control or traditional neural network-based adaptive control, these approaches are fundamentally "reactive" feedback control frameworks. They primarily rely on historical and current error information for decision-making and lack predictive, forward-looking insight into the future dynamics of the system. Consequently, their overall performance in suppressing overshoot and reducing settling time remains constrained by inherent limitations [36–38]. In recent years, hybrid control strategies that combine MPC with neural networks have attracted growing attention for handling nonlinear and time-varying industrial systems. For instance, authors in [39] introduced a neural-network predictive controller based on an improved Temporal Pattern Attention Long Short-Term Memory (TPA-LSTM) model for nonlinear thermal systems, demonstrating improved tracking performance under disturbances. In [40], a process-model-free MPC-PID hierarchical control strategy was proposed, applied to a thermal power plant subsystem, pointing out the challenges of applying conventional MPC to coal-fired units with frequent load fluctuations. In [41], an economic MPC scheme for thermal-power boiler–turbine systems was further developed, framing the BTG control problem as a multi-variable optimization task under operational constraints. These studies highlight the growing research trend of integrating predictive optimization with data-driven neural-network adaptation to improve control precision and robustness in complex power systems. To fundamentally overcome the inherent limitations of the aforementioned control strategies, MPC is regarded as an ideal approach for managing complex industrial processes, owing to its distinctive advantages of online rolling optimization, explicit constraint handling, and prediction of future system dynamics [42]. In recent years, the integration of MPC with other intelligent algorithms has emerged as a prominent research focus in the field of advanced control. Employing the MPC algorithm as an optimization mechanism to guide the tuning of neural network PID parameters provides an effective approach for enhancing the control performance of complex systems [43, 44].

Based on the analysis and synthesis of the aforementioned studies, this paper aims to address the inherent trade-off in traditional PID and single neural network PID controllers between rapid response and overshoot suppression due to their lack of predictive capability, as well as the technical challenge of reduced robustness in standalone MPC control. By leveraging the global planning capability of MPC through online rolling optimization and the local tracking advantage of neural network PID nonlinear adaptive control, this study integrates the two approaches to propose a hierarchical control strategy combining MPC with neural network PID. This strategy ultimately achieves comprehensive optimal control of the power output of coal-fired power generation units. Specifically, this study constructs a nonlinear dynamic model of the boiler–turbine–generator system based on a 660 MW coal-fired power plant and designs a neural network PID control structure with MPC serving as the external optimizer. This approach effectively addresses the challenge of adaptively tuning traditional PID control parameters and enhances both the flexibility and robustness of the control system. The core idea of this strategy is to use the upper-level MPC to perform globally optimal path planning and

generate a dynamic reference trajectory that is both fast and stable, while the lower level retains the BP neural network PID controller to leverage its strong nonlinear approximation and adaptive tracking capabilities to accurately follow this trajectory. This hierarchical architecture [45] is designed to decouple the traditional trade-off between speed and stability in control systems, with the ultimate goal of achieving comprehensive optimal control of the power output of coal-fired power generation units [46], with complete overall simulation modeling and verification of the system.

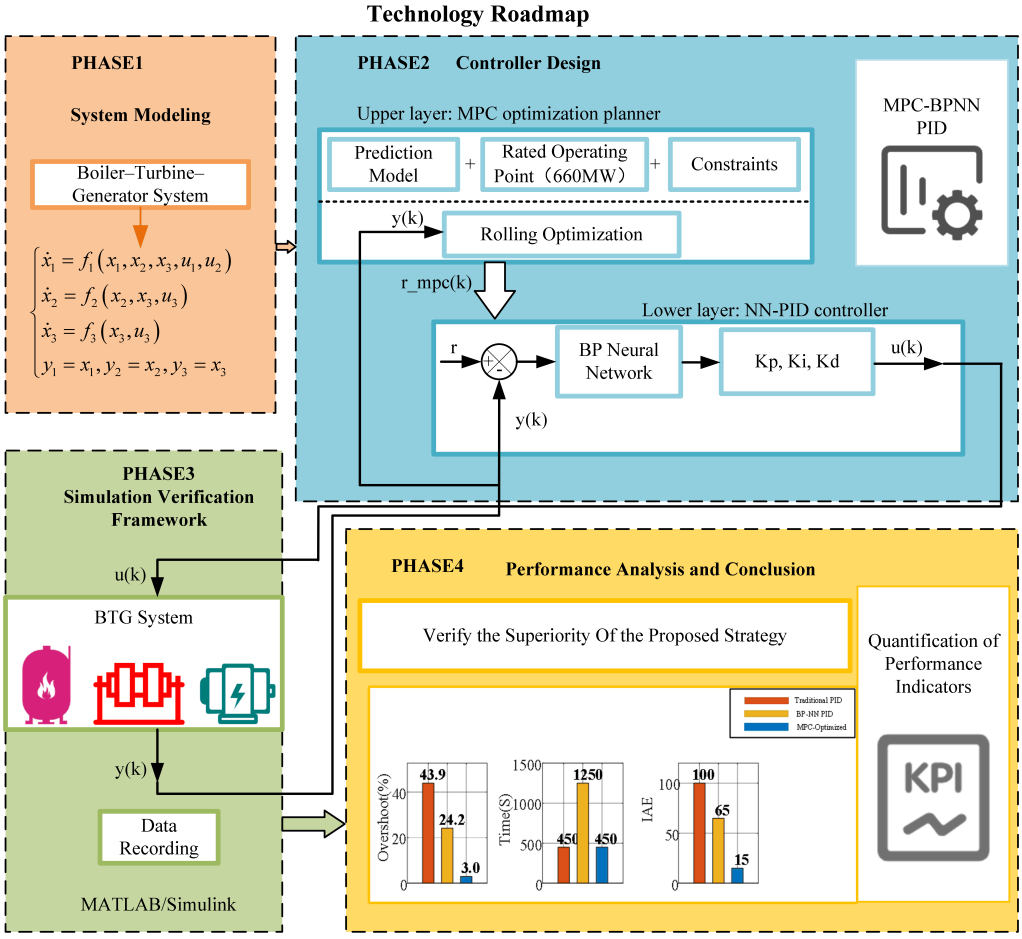

Figure 2. Technology roadmap.

The primary contributions of this study are summarized as follows:

(1) A hierarchical control architecture was designed, using upper-layer MPC for global dynamic trajectory planning and lower-layer BP neural network adaptive tuning PID controllers to track the trajectory, thereby achieving fast response and high stability in coordinated control and overcoming the trade-off between response speed and stability in traditional control methods in nonlinear systems.

(2) Introducing MPC for time-domain prediction and real-time feedback optimization of its control output, while retaining the strong nonlinear modeling and adaptive advantages of neural networks, enhances the system's predictive control capabilities, effectively reducing overshoot, steady-state error, and settling time, and improving overall dynamic performance.

(3) Taking actual-scale coal-fired power generation units as the research object, a nonlinear dynamic model integrating the boiler, turbine, and generator was constructed on the MATLAB/Simulink platform. The system verified the significant advantages of the proposed control strategy in terms of multiple performance indicators (such as overshoot, response time, and steady-state error), indicating that this method has good engineering feasibility and promotion value.

The remaining chapters are organized as follows: Section 2 presents the research methodology adopted in this study. Section 3 establishes the mathematical model of the controlled object, namely a coal-fired power plant generator set. Section 4 develops the proposed MPC–BP–NN–PID control framework and details its parameter optimization mechanism. Section 5 performs extensive MATLAB/Simulink simulations to validate the proposed strategy, including analyses of computational complexity and real-time feasibility, sensitivity analysis, a comparative discussion with other advanced control strategies, and robustness and denoising performance evaluation. Finally, Section 6 concludes the study and outlines potential directions for future research.The technical route is shown in Figure 2.

Table 1. Comparison of advanced PID control algorithms.

Method	**Main ideas**	**Advantages**	**Limitations**	**Applicable scenarios**
Traditional PID	Fixed PID gain	Simple and easy	Poor adaptability	Linear gradual change system
Self-tuning PID	Online parameter adjustment	Highly adaptable	Dependency identification	Time-varying system
Fuzzy PID	Fuzzy reasoning	Highly robust	Design dependencies	Uncertain nonlinear systems
Neural network PID	Self-learning	Nonlinear adaptation	Difficult training	Strongly coupled system
MPC optimized PID	Predictive optimization	Multivariable control	Model complexity	Large time-delay system
Fuzzy neural network PID	Integrated learning	Strong robustness	Complex design	Nonlinear dynamic systems

2. Research methods

The 660 MW generator set system of coal-fired power plants presents many control challenges, such as multiple variables, strong coupling, and complex dynamic characteristics. Although traditional PID control has a simple structure, it is difficult to adjust parameters under conditions of large time delays, large inertia, and dynamic load changes. It also has limited adaptability and is prone to large steady-state errors or severe overshoot. Therefore, advanced PID control is required. The advanced PID control algorithms are compared in Table 1.

Considering the multivariable, strongly coupled, large-inertia, and dynamically varying characteristics of coal-fired power plant generator sets, this study adopts a neural network PID control strategy optimized by MPC, which effectively balances predictive capability, adaptive tuning, and the handling of complex constraints.

2.1. BP neural network PID

As control systems become increasingly complex, traditional PID controllers have gradually exhibited limitations such as insufficient control accuracy, difficulty in parameter tuning, and poor adaptability when applied to nonlinear, time-varying, and high-delay industrial processes [47]. To enhance the intelligence and adaptive capabilities of controllers, researchers have proposed a neural network PID control strategy that integrates artificial neural networks (ANN) with PID controllers. Among these, the Back Propagation neural network, owing to its clear structure, mature training methods, and strong generalization ability, has been widely applied for online PID parameter adjustment and nonlinear modeling control [48].

A Backpropagation Neural Network (BPNN) is a typical feedforward multilayer perceptron (MLP), consisting of an input layer, one or more hidden layers, and an output layer. The network propagates input information through nonlinear activation functions layer by layer and employs the backpropagation algorithm to iteratively adjust connection weights and biases, minimizing the error between the actual output and the desired value [49]. This learning mechanism endows BPNN with strong self-learning, adaptive, and nonlinear approximation capabilities, allowing it to effectively capture complex mapping relationships between input data and system outputs. Consequently, it facilitates higher-precision modeling and control of target systems in various control tasks.

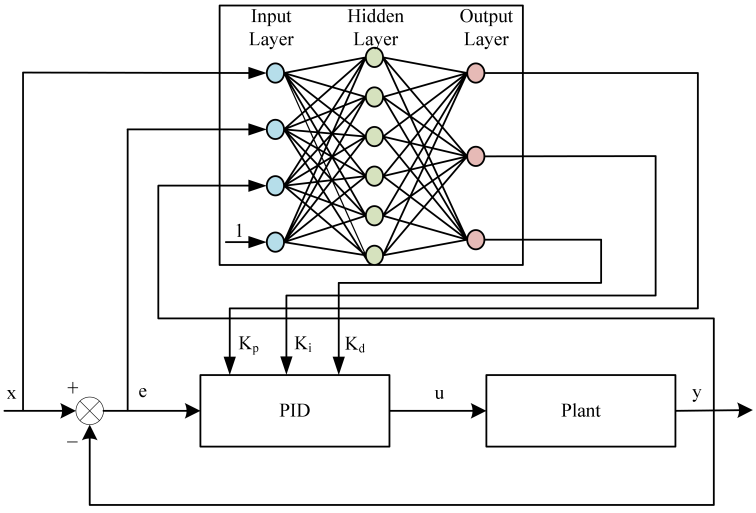

Figure 3. BP neural network PID control system structure diagram.

Therefore, in this study, the BP neural network was chosen as the core model for the neural network PID controller to enhance its self-learning, adaptive, and robust capabilities, thereby meeting the complex control requirements of coal-fired power generation units, which are nonlinear, high-inertia, and time-varying. The structure of the BP neural network PID control system is illustrated in Figure 3.

2.2. *Model predictive control (MPC)*

MPC is particularly well-suited for controlling multi-input multi-output (MIMO) systems, systems with significant constraints (such as actuator saturation and output limits), and systems with large inertia and long time delays. In the boiler–turbine–generator system of a coal-fired power plant, the system's complex structure, strong variable coupling, and frequent changes in operating conditions make MPC an effective approach. It can predict the system's dynamic response based on the model and efficiently handle input-output constraints while maintaining control performance, thus becoming a key research focus in advanced control for thermal power systems [50, 51]. Furthermore, with the development of intelligent algorithms and optimization theory, MPC has increasingly been integrated with intelligent control technologies such as neural networks, fuzzy systems, and genetic algorithms. This integration has been applied to model identification, adaptive control, and controller structure optimization, continuously enhancing MPC's application potential in coal-fired power generation control systems [52].

MPC is an advanced control strategy based on rolling optimization using a system dynamic model. Since its introduction in the 1970s, MPC has been widely applied in industrial process control systems such as chemical engineering, power generation, and energy systems, where high demands for dynamic performance and constraint handling exist [53]. The fundamental principle of MPC involves predicting the system's output behavior over a future time horizon using the mathematical model of the controlled object at each control time step. An optimization algorithm is then used to determine a sequence of control actions that maximize a performance metric. Only the first control action in the sequence is implemented at the current time step, after which the prediction is updated and the optimization process is repeated in a rolling manner.

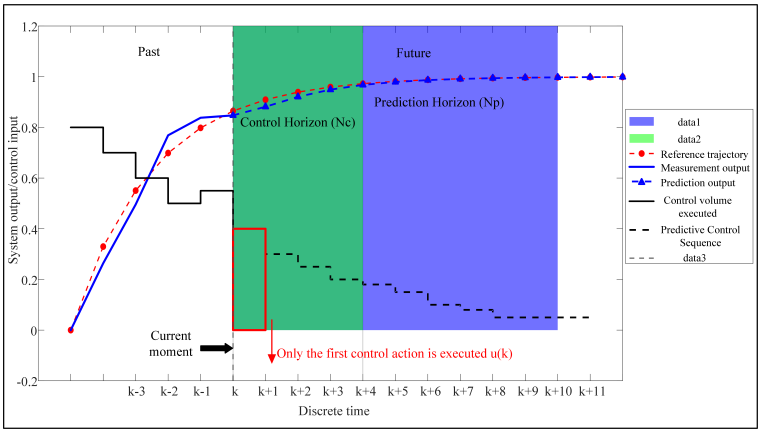

Figure 4. MPC schematic diagram.

The core components of MPC include a predictive model, a performance metric function, and a rolling optimization mechanism. First, the system model is used to predict the output trajectory over the next N_p control steps. Second, the performance metric function typically employs a weighted quadratic objective function to balance tracking error and control input variations. Finally, the rolling optimization strategy recalculates the control input at each sampling instant, ensuring that the system maintains robustness and stability under complex conditions such as disturbances, constraints, and time-varying parameters. The principle is illustrated in Figure 4.

3. System modeling

To achieve effective control of the 660 MW coal-fired power plant generating units, it is first necessary to establish a mathematical model that captures their primary dynamic characteristics. Following commonly used dynamic modeling approaches for thermal power plant units [54], the BTG system is physically decoupled into three interconnected subsystems. The overall structure and signal flow relationships are illustrated in Figure 5.

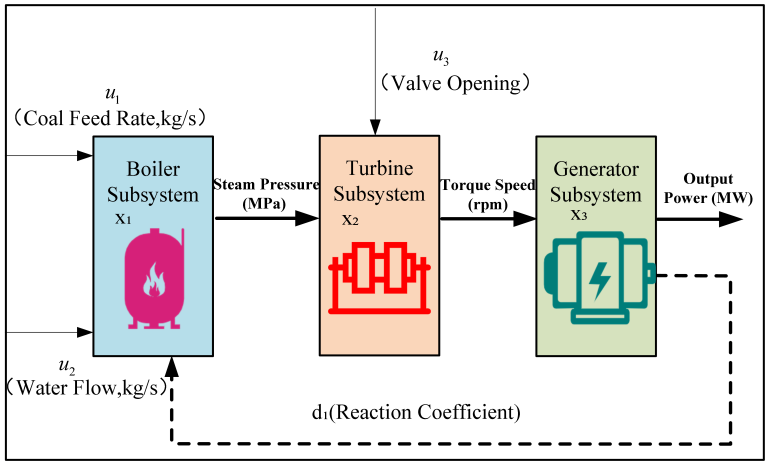

Figure 5. System structure and signal flow diagram.

The system is a typical three-input, three-output nonlinear coupled system and can be represented by a set of state equations in the form shown in Equation (3.1).

$$\begin{cases} \dot{x}_1 = f_1(x_1, x_2, x_3, u_1, u_2) \\ \dot{x}_2 = f_2(x_2, x_3, u_3) \\ \dot{x}_3 = f_3(x_3, u_3) \\ y_1 = x_1, y_2 = x_2, y_3 = x_3 \end{cases} \tag{3.1}$$

The three inputs of the system are the coal feed rate, water flow rate, and steam valve opening, while the three outputs are the main steam pressure, turbine speed, and generator power. A mathematical description of the dynamic characteristics of each subsystem is provided below. During the modeling process, the following assumptions are made: The dynamics of each subsystem within the sampling period are represented by first-order differential equations. High-frequency disturbances and extreme accident conditions are neglected, and only normal load regulation and fuel fluctuation scenarios are considered.

3.1. Boiler subsystem model

The boiler is modeled using a zero-dimensional (lumped-parameter) approach, following the methodology presented in [55]. This modeling choice is primarily due to the lack of detailed data on temperature distribution within the furnace, while also maintaining model simplicity. Heat transfer is considered primarily through radiation, with convective heat transfer effects neglected [56]. The flue

gas composition is calculated assuming a 20% excess air ratio at full load, based on the stoichiometric combustion reactions of carbon, hydrogen, and sulfur in the coal, while other components, such as nitrogen and moisture, are treated as inert.

The dynamic behavior of the furnace gas temperature is described using the energy conservation equation, whereas the mass conservation equation adopts a steady-state assumption, as the gas flow can respond rapidly to changes in inlet conditions [57]. The energy balance is expressed in Equation (3.2).

$$\dot{m}_{\text{coal}}(\text{NCV}_{\text{coal}} + h_{\text{coal}}) + \dot{m}_{\text{air}}h_{\text{air}} - \dot{m}_{\text{gas}}h_{\text{gas}} - \dot{m}_{\text{ash}}h_{\text{ash}} - Q_R = V_{F\rho g}\frac{dh_g}{dt} \tag{3.2}$$

The radiation heat transfer Q_R in the furnace chamber is described by Equation (3.3).

$$Q_R = k\sigma V_F T_g^4 \cdot \frac{1}{\rho_g}, \tag{3.3}$$

where k denotes the radiation correction coefficient, which accounts for the effects of furnace geometry, flue gas composition, absorption rate, and other influencing factors on radiative heat transfer. σ is the Stefan–Boltzmann constant, a fundamental constant used in radiant heat calculations. V_F is the furnace effective radiation volume, representing the spatial domain participating in radiative heat transfer. T_g denotes the effective gas temperature in the furnace. The fourth power relationship highlights the strong dependence of radiative power on temperature, as described by the blackbody radiation law. The effective gas temperature T_g in the furnace is calculated using Equation (3.4).

$$T_g = \beta T_{g,ad} + (1-\beta)T_{\text{FEGT}}, \tag{3.4}$$

where β is a weighting coefficient (ranging from 0 to 1) representing the influence of furnace radiation heat transfer and combustion conditions on the final flue gas temperature. $T_{g,ad}$ denotes the adiabatic flue gas temperature, representing the theoretical temperature of the flue gas after fuel combustion under the assumption of no heat loss. It reflects the ideal scenario in which the chemical energy released during combustion is fully converted into the thermal energy of the flue gas. T_{FEGT} denotes the furnace exit gas temperature, representing the actual flue gas temperature at the furnace outlet, accounting for effects such as radiation heat transfer and heat losses.

The left-hand side of the energy balance equation represents energy inflow, outflow, and losses, whereas the right-hand side denotes the rate of energy change within the boiler. The energy supplied by the fuel (coal) is divided into two components: NCV_{coal} , the lower heating value, corresponding to the heat released by chemical combustion reactions, and h_{coal} , the coal enthalpy, representing the energy associated with its physical state. $\dot{m}_{air}h_{air}$ is the physical enthalpy contributed by the air entering the boiler, primarily due to its temperature. $\dot{m}_{gas}h_{gas}$ is the enthalpy carried away by the flue gas (combustion products) exiting the boiler, representing an energy loss. $\dot{m}_{ash}h_{ash}$ is the physical enthalpy carried away by fly ash and furnace slag, which also constitutes an energy loss. Q_R represents other heat losses, such as convective and radiative losses. V denotes the furnace volume, F the volume fraction (gas fill ratio), ρg the furnace gas density, and h_g the specific enthalpy of the furnace gas. Physically, variations in the temperature and enthalpy of the gas within the boiler result in accumulation or depletion of internal energy.

The furnace model described above characterizes the key physical processes on the boiler's fire-side. However, for the control and operation of the entire power generation unit, the focus should be on

the macro-dynamic response of the boiler as a whole. The boiler's ultimate output is high-temperature, high-pressure steam, whose energy state is primarily reflected by the main steam pressure, serving as the critical link between the boiler's heat generation and the turbine's steam consumption. Therefore, based on the thermodynamic model developed in this study, a dynamic model of the boiler subsystem was further constructed, with the main steam pressure as the core state variable.

The core function of the boiler subsystem is to heat the working fluid (feedwater) and convert it into high-temperature, high-pressure steam with specific parameters (temperature and pressure) through fuel (coal) combustion. In this model, the main steam pressure x_1 is treated as the key variable representing the boiler's energy storage state. Its dynamic behavior is described by Equation (3.5).

$$\dot{x}_1 = -a_1 \cdot x_1 + b_1 \cdot u_1 - c_1 \cdot u_2 - d_1 \cdot x_3 \tag{3.5}$$

This equation illustrates the dynamic equilibrium mechanism of the main steam pressure in the boiler. $a_1 \cdot x_1$ denotes the intrinsic pressure dissipation of the boiler system, reflecting the natural downward trend in pressure due to factors such as heat loss. $b_1 \cdot u_1$ represents the positive gain effect of the coal feed rate on the main steam pressure. An increase in fuel input directly enhances the boiler's evaporation rate, resulting in a pressure rise in the boiler. indicates the negative inhibitory effect of the boiler feedwater flow on main steam pressure, as the injection of low-temperature feedwater absorbs heat from the boiler's water-cooled walls, causing an instantaneous disturbance in steam pressure. $d_1 \cdot x_3$ describes the feedback effect of generator power (i.e., load) variations on boiler pressure. When external load demand x_3 increases, steam consumption accelerates, generating a negative feedback on boiler pressure.

3.2. Turbine subsystem model

The dynamic model of the steam turbine is based on the volumetric form of Stodola's elliptical law [58], which is applicable to all compressible fluid conditions. In the modeling process, the turbine shaft speed is assumed constant, and leakage flow is neglected. Since the response of the steam turbine is much faster than that of the boiler, a steady-state model is employed. The steam mass flow rate is given by Equation (3.6).

$$\dot{m}_{in} = \frac{K_{SE}}{\sqrt{v_{in}}} \sqrt{\frac{P_{in}^2 - P_{out}^2}{P_{in}}}, \tag{3.6}$$

where K_{SE} is the flow coefficient, V_{in} is the pressure exponent, P_{in} is the inlet pressure, and P_{out} is the outlet pressure. The inlet and outlet temperatures are given by Equation (3.7).

$$\frac{T_{out}}{T_{in}} = \left(\frac{P_{out}}{P_{in}}\right)^{\left(\frac{\gamma-1}{\gamma}\right)}, \tag{3.7}$$

where T_{out} denotes the outlet temperature, T_{in} the inlet temperature, and γ the specific heat ratio, which is approximately 1.4 for air.

To characterize this energy conversion process and its effect on system dynamics, it is necessary to establish the dynamic relationship among the throttle valve opening as the control input, the steam flow as the energy input, and the turbine speed as the system output.

The primary function of a steam turbine is to efficiently convert the thermal energy of steam into mechanical work that drives the generator. Its dynamic behavior is mainly represented by variations

in rotational speed x_2, which are directly governed by the steam flow entering the turbine. The steam flow, in turn, is determined by the opening of the speed control valve u_3. The dynamic equation is given by Equation (3.8).

$$\dot{x}_2 = -a_2 \cdot x_2 + b_2 \cdot u_3 \cdot x_1, \tag{3.8}$$

where $a_2 \cdot x_2$ denotes the turbine rotor speed loss term, primarily arising from mechanical friction, aerodynamic resistance, and other factors. $b_2 \cdot u_3$ represents the gain of the speed control valve opening on turbine speed; an increase in valve opening raises the steam flow, thereby enhancing the turbine's output torque and rotational speed.

3.3. Generator subsystem model

The generator is mechanically coupled to the turbine on the same shaft, so its rotational speed is dictated by the turbine's output speed. The generator's electrical frequency f is related to its rotational speed N_{rpm} and the number of pole pairs N_p, as given by Equation (3.9).

$$f = \frac{N_{rpm} \cdot N_p}{120} \tag{3.9}$$

Equation (3.9) illustrates the direct kinematic implication of the coaxial coupling between the generator and the turbine, namely that the grid frequency is uniquely determined by the mechanical speed. The fundamental purpose of this physical connection, however, is energy conversion. Based on this kinematic relationship, the core function of the generator, converting input mechanical energy into electrical energy, is further modeled. The generator's active power output x_3 is directly dependent on the turbine-provided rotational speed x_2, and its dynamic equation is given by Equation (3.10).

$$\dot{x}_3 = -a_3 \cdot x_3 + b_3 \cdot x_2, \tag{3.10}$$

where $a_3 \cdot x_3$ represents the dissipative effect of the power system load on the generator's active power, reflecting intrinsic losses in the electrical system. $b_3 \cdot x_2$ denotes the conversion efficiency from turbine rotational speed to generator active power, capturing the fundamental electromagnetic energy conversion relationship: higher input speed results in higher output power.

3.4. Model parameter summary

The physical significance of all key parameters in the above model and the specific values used in this simulation study are shown in Table 2.

Table 2. Key parameters of the system model and their physical significance.

Parameters	Physical meaning	Simulation value
a_1	Boiler pressure natural loss coefficient	-0.04
b_1	Pressure gain per coal feed rate	0.05
c_1	Feedwater flow suppression on main steam pressure	-0.08
d_1	Reaction coefficient of generator power on boiler pressure	-0.005
a_2	Turbine speed natural loss coefficient (such as friction)	-0.03
b_2	Gain coefficient of valve opening to turbine speed	0.035
a_3	Load dissipation factor of generator power	-0.01
b_3	Turbine speed-to-power conversion efficiency	0.066

3.5. Application analysis of model characteristics in control systems

The mathematical model developed in this section not only accurately captures the primary dynamic characteristics of the boiler–turbine–generator system in a 660 MW coal-fired power plant but also provides a solid theoretical and engineering foundation for the subsequent controller design.

First, the model is formulated in a state-space representation, which directly satisfies the structural requirements of MPC for predictive models, allowing the controller to accurately compute the optimal control sequence within a finite prediction horizon. Second, all key parameters in the model possess clear physical significance and tunability, facilitating offline calibration during the design phase as well as online parameter identification and adaptive optimization during operation, thereby enhancing the robustness and adaptability of the control system. Furthermore, the model provides a quantifiable training objective and real-time feedback pathway for the neural network PID controller, enabling incremental learning from both historical and current system responses and dynamically optimizing control gains. More importantly, the model exposes significant nonlinearities and multivariable coupling characteristics, highlighting the inherent performance limitations of conventional single-linear control strategies under complex operating conditions such as load disturbances and fuel fluctuations. This lays a solid theoretical and structural foundation for implementing a joint BP neural network + MPC control strategy.

4. Controller design

The design of the controller is a key determinant of power regulation performance in coal-fired power plant generating units, directly influencing operational efficiency, stability, and economic viability. Considering the inherent limitations of conventional PID controllers in handling complex systems such as coal-fired units, characterized by pronounced nonlinearity, strong coupling, and

substantial time delays, this section develops a composite controller that combines neural network–based adaptive regulation with model predictive optimization.

This strategy implements a hierarchical intelligent control framework. The lower layer employs a NN-PID controller, exploiting the nonlinear mapping and self-learning capabilities of neural networks to enable online dynamic tuning of PID parameters, thereby addressing local nonlinearity and time-varying characteristics of system parameters. The upper layer integrates MPC, utilizing its predictive multi-step forecasting and rolling optimization to globally optimize setpoint trajectories and critical system parameters, effectively handling multi-variable coupling and operational constraints. This hierarchical design systematically addresses the control challenges inherent in coal-fired power plants, yielding substantial improvements in control accuracy and dynamic response performance.

4.1. Structural design of neural network PID controller

To effectively mitigate the nonlinear dynamics inherent in coal-fired power generation units, the lower-level control loop of this strategy utilizes a BP (backpropagation) NN-PID controller. In this controller, the fixed proportional (k_p), integral (k_i), and derivative (k_d) gains of a conventional PID are replaced by a BP neural network, which performs real-time identification and adaptive tuning via online learning. This configuration endows the controller with enhanced adaptability to system nonlinearities, parameter variations, and external disturbances.

The BP neural network built into the controller uses a three-layer structure with the following specific configuration:

(1) **Input layer:** Contains four nodes, whose input signals are: normalized power setpoint $r(k)$, normalized actual power output $y(k)$, normalized output error $e(k)$, and a constant offset term of 1.
(2) **Hidden layer:** Contains six nodes, and the activation function uses the hyperbolic tangent function (tanh), because its S-shaped curve characteristics and output centered on the origin provide faster convergence speed and stronger nonlinear mapping capabilities.
(3) **Output layer:** Contains three nodes, corresponding to the three original gains of the PID. The activation function uses the sigmoid function, which smoothly constrains the output value within the range (0, 1), facilitating subsequent normalization parameter scaling and ensuring the physical significance and stability of the output gain.

The controller employs an incremental PID algorithm, which mitigates integral windup and ensures that the computation of the control action depends solely on the errors from the most recent sampling cycles. The calculation of the control increment $\Delta u(k)$ at the current step is given by Equation (4.1).

$$\begin{aligned}\Delta u(k) = {} & k_p(k) \cdot [e(k) - e(k-1)] + k_i(k) \cdot e(k) \\ & + k_d(k) \cdot [e(k) - 2e(k-1) + e(k-2)],\end{aligned} \tag{4.1}$$

where $k_p(k)$, $k_i(k)$, and $k_d(k)$ represent the dynamic gains output in real time by the BP neural network at current time step k . The control signal applied to the actuator (valve) is obtained by integrating the control increment, as given by Equation (4.2).

$$u_3(k) = u_3(k-1) + \Delta u(k) \tag{4.2}$$

To ensure smoother actuator (valve) commands, prevent mechanical wear, and suppress system oscillations, the computed control increment $u_3(k)$ was processed through a first-order low-pass filter, with upper and lower limits set to 0–150. The neural network weights are updated using the gradient descent method, aiming to minimize the system output error $e(k)$. The control error is defined by Equation (4.3).

$$E(k) = \frac{1}{2}(r(k) - y(k))^2 \tag{4.3}$$

where $r(k)$ and $y(k)$ represent the reference signal and the system output at time k, respectively. The weights and biases of the network are updated in real time according to the gradient descent rule by Equation (4.4).

$$w_{ij}(k+1) = w_{ij}(k) - \eta \frac{\partial e(k)}{\partial w_{ij}} + \alpha[w_{ij}(k) - w_{ij}(k-1)], \tag{4.4}$$

where w_{ij} represents the connection weight between neuron i and neuron j. The error backpropagation process ensures that neurons with greater contribution to output error receive larger gradient corrections, thereby accelerating convergence while maintaining system stability. The output layer of the network provides real-time corrections to the proportional, integral, and derivative coefficients, which can be expressed as Eqs. (4.5)–(4.7).

$$k_p(k) = k_{p0} + \Delta k_p(k) \tag{4.5}$$

$$k_i(k) = k_{i0} + \Delta k_i(k) \tag{4.6}$$

$$k_d(k) = k_{d0} + \Delta k_d(k), \tag{4.7}$$

where k_{p0}, k_{i0}, and k_{d0} are the initial PID parameters determined by the nominal model or manual tuning, while $\Delta k_p(k)$, $\Delta k_i(k)$, and $\Delta k_d(k)$ are the dynamic corrections generated by the BP neural network based on the current input vector in Equation (4.8).

$$X(k) = [e(k), \dot{e}(k), \int e(k)] \tag{4.8}$$

Once the PID parameters are obtained from the neural network output layer, the control signal $u(k)$ is calculated according to the incremental PID control law by Equation (4.9).

$$u(k) = k_p(k)e(k) + k_i(k)\sum_{j=0}^{k} e(j) + k_d(k)[e(k) - e(k-1)] \tag{4.9}$$

This expression describes the feedforward control action generated at each sampling instant, which drives the plant toward the desired output. Key parameter settings during the learning process are as follows: the learning rate is set to 0.005, with a lower value ensuring stable convergence. The momentum factor is set to 0.01, where the inclusion of the momentum term helps the algorithm to overcome local minima in the error surface and accelerates convergence. The algorithm flow of the controller is shown in Figure 6.

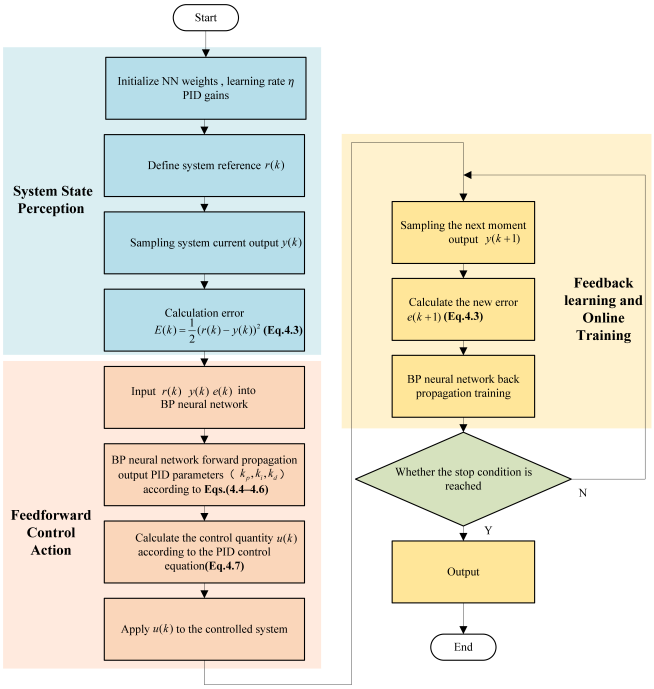

Figure 6. Flowchart of neural network PID algorithm.

4.2. MPC module design

Although the BP neural network PID controller performs well in handling nonlinearity and uncertainty, it fundamentally operates as a model-free feedback controller. When dealing with multivariable systems such as coal-fired power plant units, which are characterized by strong coupling, multiple constraints, and high inertia, its purely reactive nature limits predictive capability. To overcome this limitation, a MPC module is introduced as the upper-level optimization layer of the proposed control framework.

MPC explicitly utilizes a system prediction model to forecast future process behavior within a finite prediction horizon. At each sampling instant, it solves an optimization problem to determine the control sequence that minimizes the predicted tracking error while satisfying physical and operational constraints. Only the first control action is implemented, and the optimization is repeated in the next cycle, forming a rolling (receding) horizon optimization mechanism.After describing the general mechanism of MPC, the next steps involve outlining the specific components that define the model and optimization process for the given system. These include:

(1) Prediction model construction. The original nonlinear dynamics of the 660 MW BTG system are simplified into an observable second-order prediction model, focusing on the dominant control chain from the valve opening u_3 to generator power output y. The prediction model is described by Eqs. (4.10) and (4.11).

$$x_1(k+1) = a_1 x_1(k) + b_1 u_3(k) \tag{4.10}$$

$$y(k+1) = a_2 x_1(k+1) + b_2 u_3(k) \tag{4.11}$$

This discrete-time model retains the essential input–output dynamics for MPC prediction while ensuring numerical stability and computational efficiency.

(2) Optimization objective function. At each time step, MPC predicts the future output trajectory over the prediction horizon N_p and computes the optimal PID gain sequence by minimizing the quadratic performance index. As given by Equation (4.12), the objective function minimizes the quadratic performance index of tracking error and control input changes.

$$J = \sum_{i=1}^{N_p} [y_{ref}(k+i) - \hat{y}(k+i|k)]^2 + \lambda \sum_{i=1}^{N_c} [\Delta u(k+i-1)]^2, \tag{4.12}$$

where y_{ref} is the reference output (power setpoint), Δu is the control increment, N_p is the prediction horizon, N_c is the control horizon, and λ is a penalty factor to balance response speed and smoothness. A small λ leads to faster tracking but larger overshoot, while a larger λ ensures smoother actuator motion and system stability.

(3) Constraints handling. To ensure safe and realistic operation, MPC explicitly incorporates system and actuator constraints such as Equation (4.13)

$$u_{\min} \le u(k+i) \le u_{\max}, \Delta u_{\min} \le \Delta u(k+i) \le \Delta u_{\max} \tag{4.13}$$

These constraints prevent excessive valve movement, actuator saturation, and abrupt load fluctuations that could harm the generator system.

(4) Rolling optimization and parameter update. After solving the optimization problem, only the first set of optimal PID gains (k_p^*, k_i^*, k_d^*) is applied to the lower BP neural network PID controller at the current sampling instant. The system states are then updated, and the optimization is repeated at the next time step, ensuring real-time predictive adaptation. This rolling optimization structure transforms the controller from passive error correction to active predictive planning.

(5) Interaction with the BP NN-PID. The upper-layer MPC generates the optimal PID parameter sequence considering future system behavior, while the lower-layer BP neural network refines these parameters online through gradient learning to adapt to residual modeling errors and unmodeled disturbances. This predictive–adaptive collaboration significantly enhances control precision and robustness, achieving faster convergence, minimal overshoot, and superior steady-state accuracy compared with traditional and standalone BP-PID controllers.

The design of MPC is the core of this control strategy, and its main design steps are as follows: The performance of MPC strongly depends on the accuracy of its internal prediction model. Although the complete mathematical model of the controlled system is a third-order multi-input system, observability analysis reveals that the full third-order model leads to an ill-posed problem for the MPC state estimator, making it challenging to guarantee the stability and estimation accuracy of the state observer.

To ensure the robustness and practical feasibility of the MPC, a simplified, fully observable second-order core model is constructed in this study. This reduced-order model retains only the dynamic chains most directly associated with the output power $y(t)$ (i.e., x_3): u_3 (valve opening) $\rightarrow$ x_2 (turbine speed) $\rightarrow$ x_3 (generator power). In the controller design, the continuous model is discretized into a discrete-time model suitable for MPC. The MPC module flow is shown in Figure 7.

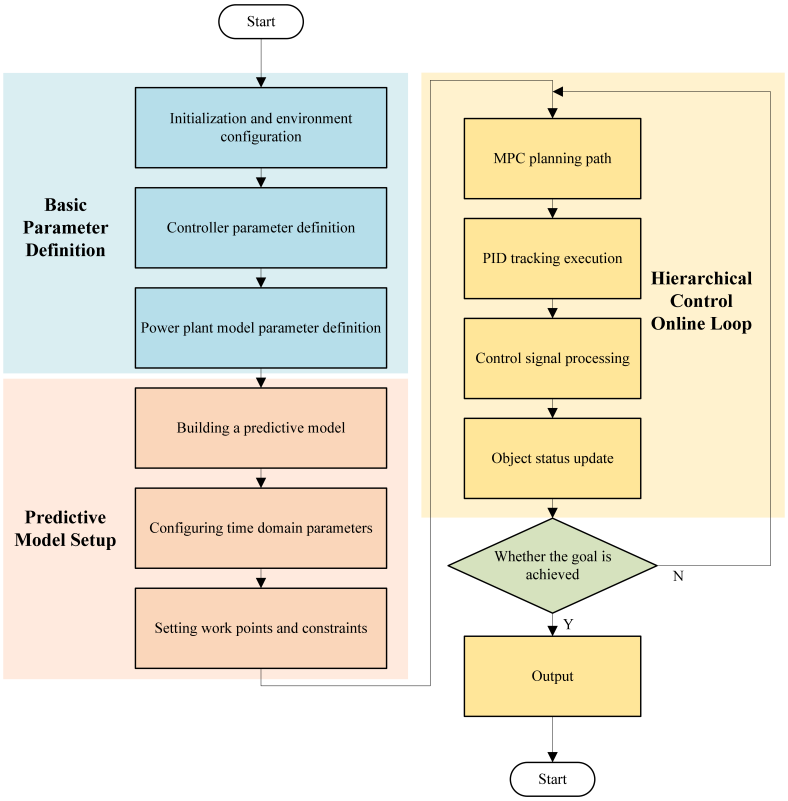

Figure 7. MPC optimization controller algorithm flowchart.

4.3. Overall framework design of the controller

To achieve efficient coordination between predictive optimization and adaptive control, this study proposes a hierarchical composite control framework that integrates MPC and a BP NN-PID controller. The overall design explicitly separates the global predictive layer (upper layer) and the local adaptive execution layer (lower layer), allowing each module to exploit its respective advantages while maintaining real-time information exchange and closed-loop coordination.

In this framework, the upper MPC module operates as a predictive optimizer based on a simplified system model. It forecasts future system dynamics within a finite prediction horizon and solves an optimization problem to obtain the optimal PID parameters minimizing predicted tracking error while satisfying actuator and operational constraints. The computed parameters represent the global control plan for the system, ensuring that the future control trajectory remains smooth and stable. The lower BP NN-PID controller receives these parameters and executes real-time control through an incremental PID strategy. Meanwhile, it updates its internal weights online by gradient learning based on the instantaneous control error, thereby refining the PID gains to compensate for modeling errors and external disturbances.

The information exchange between the two layers forms a closed predictive–adaptive loop. At the beginning of each sampling period, the MPC module predicts system behavior and outputs the optimal parameter set to the BP neural network PID controller. After executing control, the BP controller sends back the updated system states, output errors, and power response data to the MPC module. The MPC then utilizes these data for the next rolling optimization, ensuring that every cycle reflects

the latest system dynamics. Through this bidirectional flow of information, the controller maintains global foresight from MPC and local adaptability from the neural network, achieving coordinated optimization across different time scales.

The cooperative process continues in a rolling manner: MPC predicts, optimizes, and updates control parameters, while the BP neural network PID adaptively refines and implements them in real time. The feedback of system states into the next prediction horizon establishes a dynamic cycle of prediction–execution–feedback–reoptimization. This integration allows the system to dynamically balance global optimality and local adaptability, significantly improving transient response speed, reducing overshoot, and enhancing steady-state accuracy.

The overall control architecture is illustrated in Figure 8, which demonstrates the interaction between the upper MPC optimizer and the lower BP neural network PID controller. The figure clearly shows that MPC provides predictive parameter planning, the BP neural network performs adaptive fine-tuning and control execution, and real-time system feedback connects both modules into a unified control loop. This hierarchical integration effectively combines the global optimization capability of MPC with the local adaptive learning capability of the BP neural network, resulting in a coordinated and high-performance control strategy suitable for complex nonlinear power generation systems.

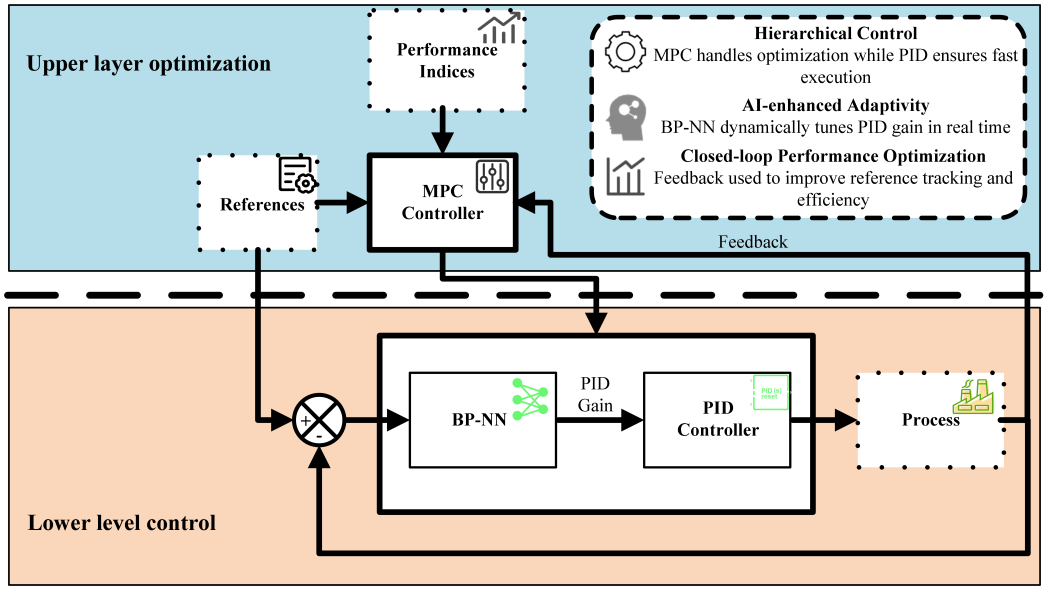

Figure 8. Control structure block diagram.

5. Experimental verification

5.1. Experimental setup and baseline performance

To validate the effectiveness of the proposed MPC-optimized NN-PID control strategy in power control of a 660 MW coal-fired power plant generator set, a complete simulation platform was established in the MATLAB/Simulink environment. The system includes a boiler–turbine–generator integrated model, based on the standard modeling structure of thermal power plants, with the input variable being "fuel flow" and the output being "power generation". The control objective is to

achieve rapid and stable tracking of the setpoint (set to 660 MW) for power generation, with fast response time, minimal overshoot, and steady-state error approaching zero.

First, based on the system modeling in Section 2, a simulation model of the boiler–turbine–generator is constructed in Simulink. The generator set model is shown in Figure 9.

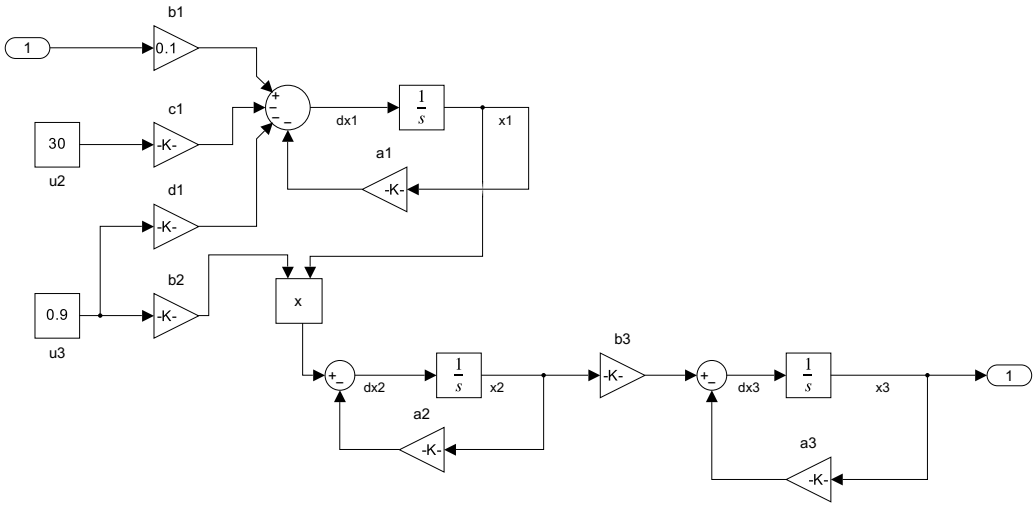

Figure 9. Generator set model diagram.

Simulation results of traditional PID control of coal-fired power plant generator sets are shown in Figure 10.

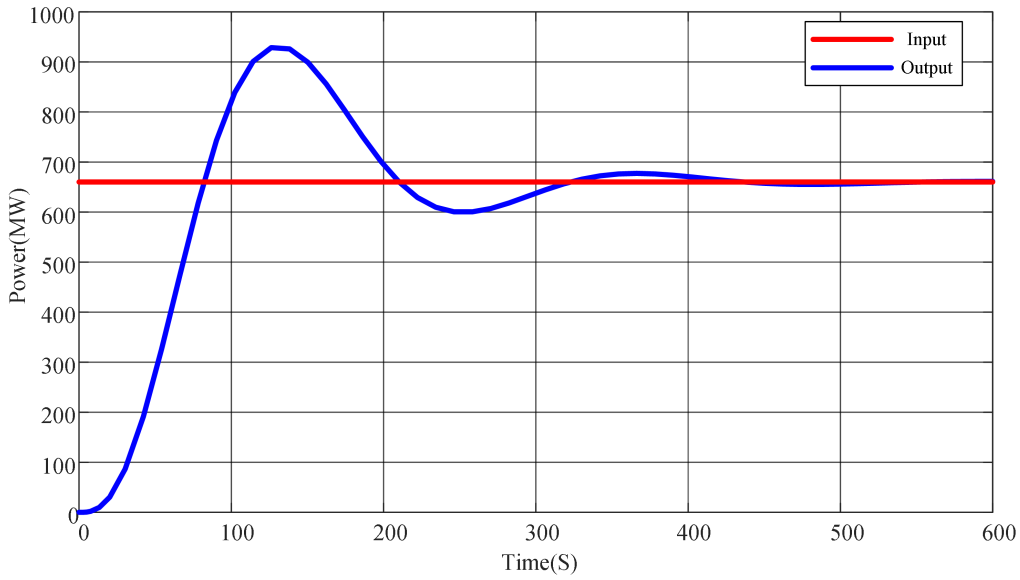

Figure 10. Traditional PID simulation results diagram.

Based on the simulation results, the system exhibits an overshoot of approximately 50%, which is relatively large. This indicates that the system overreacts to input changes, and reducing the overshoot

may require decreasing k_p or adjusting k_d. The rise time is around 100 to 150 seconds, suggesting a relatively fast response from the initial value to near the steady state. Some oscillation is observed following the overshoot, indicating underdamped behavior. Nevertheless, the steady-state error is zero, demonstrating that the PID controller successfully stabilizes the system output near the target value. Despite the oscillations before reaching steady state, the system ultimately stabilizes at the desired value of 660 MW, confirming the controller's strong steady-state tracking capability. Overall, the system responds quickly, but overshoot and transient instability remain, highlighting the need for further optimization through controller parameter tuning.

5.2. Performance of BP neural network PID controller

A PID controller based on a BP neural network was implemented using MATLAB. The PID parameters (proportional gain k_p , integral gain k_i , and derivative gain k_d) are dynamically adjusted based on the error and the historical outputs of the PID controller. By using the backpropagation algorithm for training, the code continuously optimizes the controller parameters to better control the system output. To evaluate the performance of the designed BP neural network PID controller, this paper conducted simulation experiments targeting the power step response of a generator set.

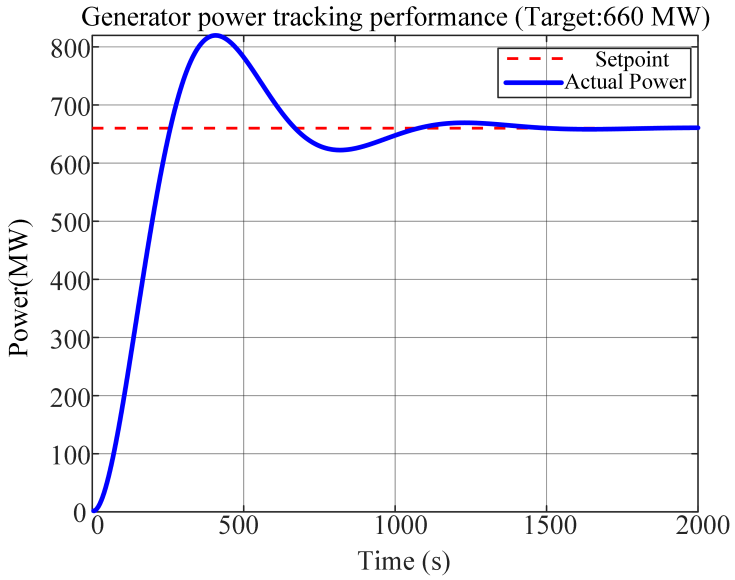

Figure 11. Power tracking performance of the standalone BP neural network PID controller for a 660 MW setpoint.

Simulation results demonstrate that the controller achieves excellent performance. As shown in Figure 11, the system output power $y_{\text{out}}(k)$ rapidly tracks the setpoint $r_{\text{in}}(k)$ without overshoot. The corresponding tracking error quickly converges to zero after a brief transient (Figure 12), indicating that the controller provides both fast dynamic response and high steady-state accuracy. During the control process, the system's internal state variables—including main steam pressure, turbine speed, and generator power—transition smoothly and eventually stabilize at new equilibrium points without significant oscillations (Figure 13), highlighting the controller's effective management of

multi-variable coupled dynamics. This superior performance is attributed to the adaptive capabilities of the neural network within the PID controller. As illustrated in Figure 14, the three PID parameters are not fixed but dynamically adjusted online by the neural network based on real-time error and system state. This intelligent parameter tuning enables the controller to efficiently accommodate the complex nonlinear characteristics of coal-fired power plants, thereby validating the feasibility and superiority of the proposed design.

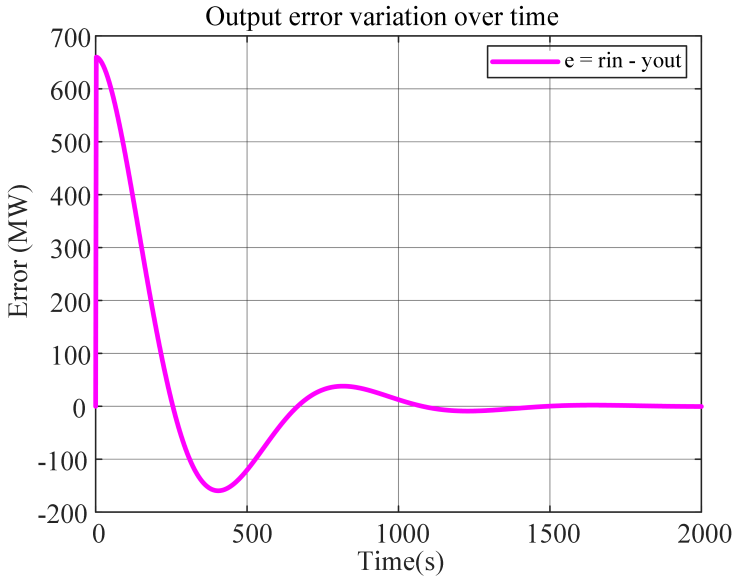

Figure 12. Error curve diagram.

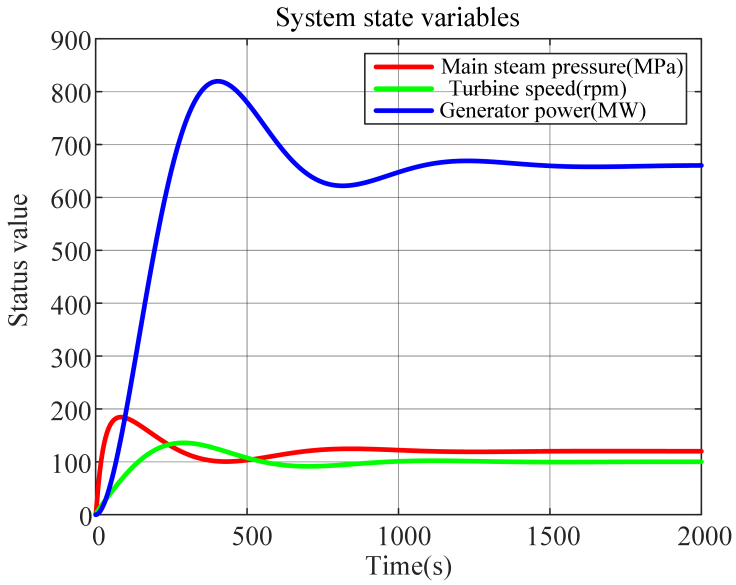

Figure 13. Dynamic response of key state variables under BP–NN PID control.

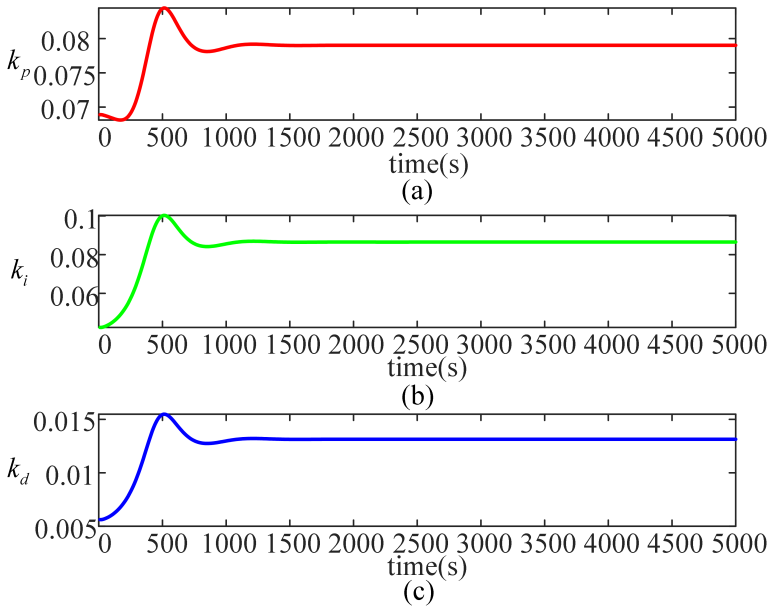

Figure 14. PID parameter change diagram (a) k_p, (b) k_i, (c) k_d.

Table 3. Comparison of traditional PID and neural network PID control simulations.

Index	**Traditional PID control**	**Neural network PID Control**	**Comparison results**
Overshoot	$\approx 44\%$	$\approx 24\%$	Overshoot is significantly reduced
Settling time	$\approx$ 450s	$\approx$ 1250s	Settling time becomes longer
Stability	There is oscillation and underdamping	Smooth convergence with little oscillation	Better stability

In summary, the introduction of the neural network PID controller has substantially improved system performance across multiple aspects. First, regarding overshoot, the system exhibited an overshoot of approximately 44% before control, which was reduced to around 24% after control, indicating effective suppression of rapid overshoot. Second, in terms of stability, the system before control showed pronounced oscillations and underdamping, whereas after control, the response was smooth with minimal oscillations, demonstrating markedly enhanced stability. However, the settling time increased from approximately 450 seconds before control to about 1,250 seconds after control, indicating that while stability improved, the response speed decreased. Overall, the neural network PID controller excels in enhancing stability and reducing overshoot, although there remains potential

for optimizing settling speed. A comparison of control performance between the traditional PID and the neural network PID is presented in Table 3.

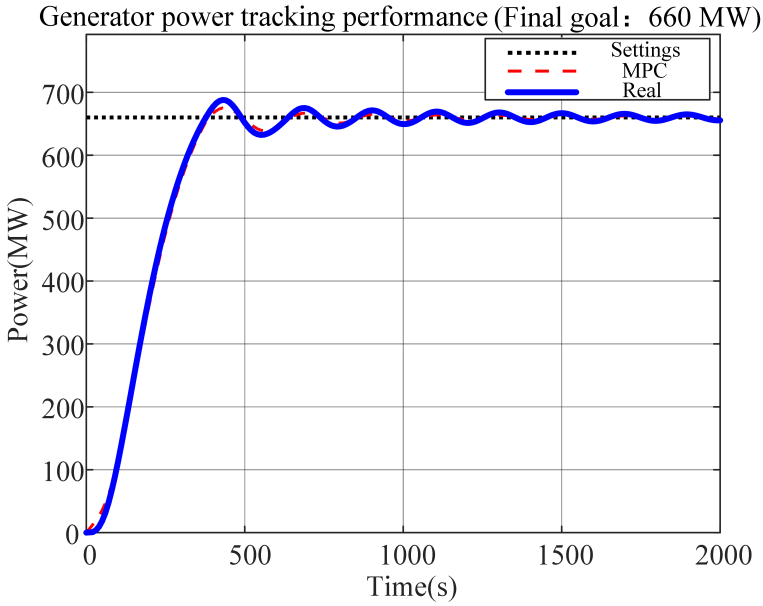

Figure 15. Power tracking performance of the proposed MPC-optimized NN-PID controller.

5.3. Performance of the proposed MPC-optimized NN-PID controller

Although the BP NN-PID controller demonstrates excellent performance in enhancing system stability and reducing overshoot, there remains potential for improvement in regulation speed. To address this, MPC is employed for upper-level optimal trajectory planning, while the lower-level BP neural network PID controller performs adaptive tracking. By defining the error signal driving neural network learning as the tracking error relative to the MPC trajectory, this approach effectively integrates the predictive capability of MPC with the nonlinear adaptive capability of the neural network. The corresponding simulation results are presented in Figures 15 to 17. The figure above provides an intuitive and quantitative comparison. Under the neural network PID control (Figure 11), although the initial response is rapid, it is accompanied by a substantial overshoot of up to 24% (peak power approximately 810 MW), which exceeds the acceptable range for industrial operation. More importantly, this pronounced overshoot induces sustained oscillations in the system, resulting in a settling time exceeding 1,200 seconds and indicating poor system stability and robustness.

In contrast, the incorporation of the MPC optimization control strategy (Figure 15) demonstrates clear performance advantages. The core of this approach is its hierarchical "predict-and-plan" structure. The upper-layer MPC controller utilizes accurate predictions of the system's future dynamics to generate an optimal reference trajectory online (red dashed line in the figure), which is both fast and free of overshoot. The lower-layer controller precisely tracks this trajectory. Simulation results show that the system's actual output power (blue solid line) closely follows the MPC trajectory, effectively eliminating overshoot. The system reaches the target value smoothly within approximately 500 seconds, reducing the settling time by more than 50% without significant

oscillations, thereby demonstrating excellent dynamic performance and stability. A comparison of control performance between the neural network PID and the MPC-optimized neural network PID is presented in Table 4.

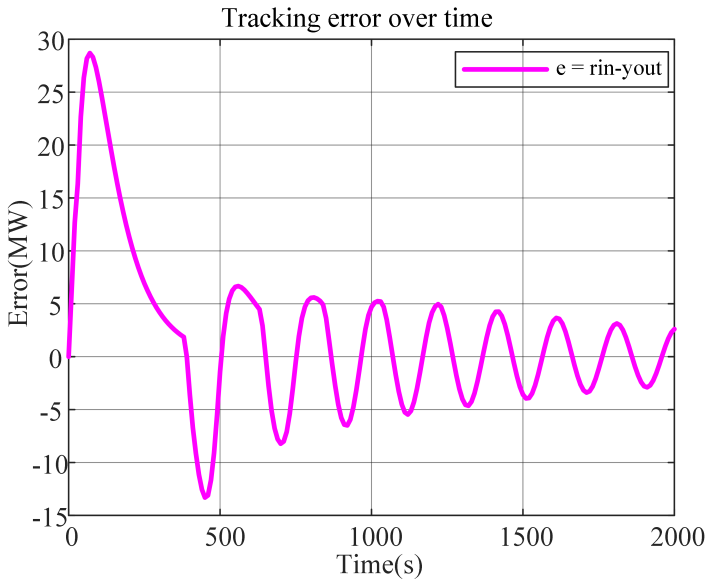

Figure 16. MPC optimization neural network PID error curve diagram.

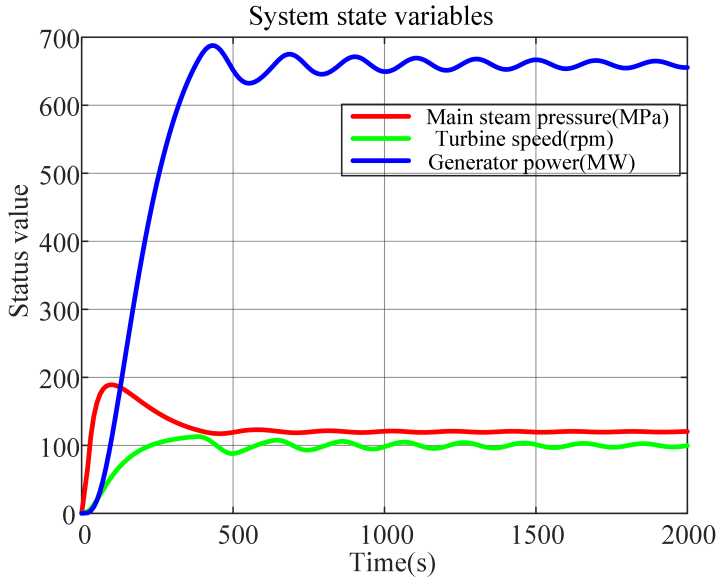

Figure 17. Dynamic response of key state variables under the proposed MPC-optimized NN-PID control.

Table 4. Comparison of neural network PID and MPC-optimized neural network PID control.

Index	Neural network PID Control	MPC optimization neural network PID	Comparison results
Overshoot	≈ 24%	≈ 3%	Significant reduction in overshoot
Settling time	≈ 1250s	≈ 450s	The settling time has been significantly reduced
Stability	Low-frequency oscillations indicate underdamping	The system remains stable with no oscillations	Better stability

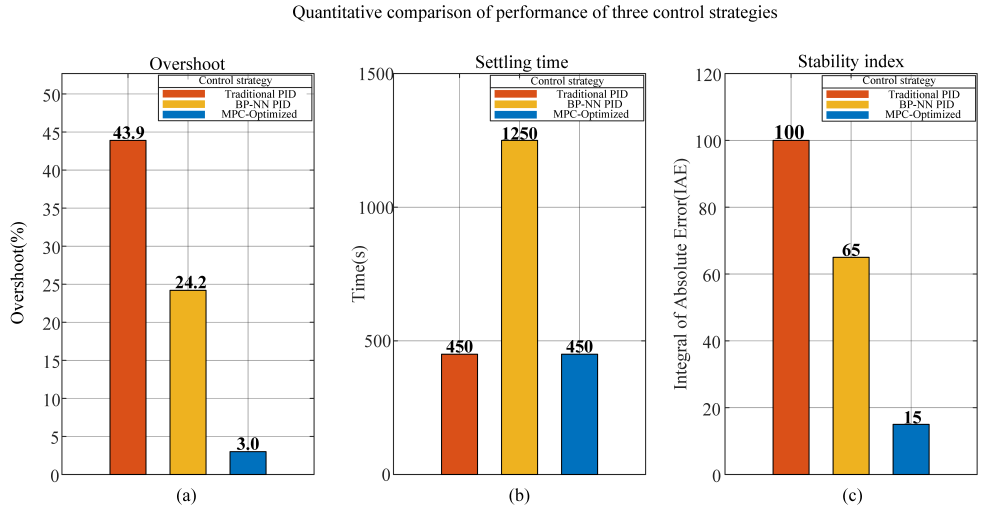

Figure 18. Quantitative comparison of the performance of the three control strategies (a) overshoot, (b) settling time, and (c) stability index.

5.4. Comprehensive comparative analysis

To provide a comprehensive and quantitative evaluation of the performance of the traditional PID controller, the BP NN-PID controller, and the MPC-optimized BP NN-PID controller proposed in this study, the dynamic responses of all three controllers were tested under a unified simulation environment. Three representative performance metrics were selected: overshoot, reflecting system stability; settling time, indicating system responsiveness; and the integral absolute error (IAE), providing a comprehensive measure of overall control error. The detailed quantitative comparison results are presented in Figure 18.

As shown in Figure 18(a), regarding system stability and overshoot, the traditional PID controller exhibits a severe overshoot of up to 43.9%, which is unacceptable in practical industrial operation and

may cause equipment damage or trigger safety protection mechanisms. The BP-NN PID controller reduces the overshoot to 24.2% through online learning, demonstrating the optimization capability of adaptive control. The MPC optimization strategy proposed in this study achieves a substantial improvement, limiting overshoot to 3.0% and approaching the ideal zero-overshoot condition. These results clearly indicate that incorporating the predictive control concept of MPC is decisive in suppressing system overshoot, with performance far exceeding that of traditional adaptive methods.

Regarding the trade-off between system speed and stability (Figure 18(b), Settling time), although the traditional PID exhibits large overshoot, its settling time is only 450 seconds. The BP-NN PID adopts a more conservative control strategy to reduce overshoot, resulting in a longer settling time of 1,250 seconds. In contrast, the MPC optimization strategy minimizes overshoot while maintaining a rapid settling time of 450 seconds. These results strongly demonstrate that the proposed hierarchical control architecture can simultaneously optimize the system's dynamic response and steady-state performance, achieving both stability and fast response without requiring a trade-off between the two.

From the perspective of the overall performance of the control process (Figure 18(c), IAE), the integral absolute error (IAE) metric comprehensively reflects the cumulative error of the entire dynamic process. The figure clearly shows a step-by-step improvement in performance: The IAE value for the traditional PID is the highest (100), followed by the BP-NN PID (65), while the IAE value for the MPC optimization strategy is the lowest, at just 15, representing a 85% reduction compared to the traditional PID and approximately a 77% reduction compared to the BP-NN PID. This indicates that the MPC optimization strategy not only performs exceptionally well in a single metric but also achieves optimal levels of overall control accuracy and robustness.

In summary, through an in-depth comparative analysis of the three core indicators–overshoot, settling time, and IAE–the advanced nature and superiority of the MPC-optimized BP neural network PID control strategy proposed in this study have been fully verified. This strategy not only addresses the significant overshoot issues of traditional control methods but also overcomes the limitations of single adaptive control, which sacrifices speed. Ultimately, it achieves fast, precise, and highly stable comprehensive optimal control of complex industrial objects, demonstrating significant advanced features and practical value.

5.5. Computational complexity and real-time feasibility

The computational complexity and real-time feasibility of the proposed MPC–NN–PID controller were evaluated through simulation tests. The MPC module employs a short prediction horizon (N_p = 10) and control horizon (N_c = 3), ensuring that the quadratic programming problem solved at each sampling period has a limited dimension and can be completed within milliseconds. In the MATLAB simulation environment, the average computation time per optimization step was below 20 ms, which is significantly shorter than the typical 1 s sampling period used in power control systems of coal-fired generator units.

The BP neural network adopts a lightweight three-layer structure with six neurons in the hidden layer, and its weight update is based on a simple gradient descent algorithm. Compared with the MPC module, its computational burden is negligible. Therefore, the proposed controller is fully capable of real-time implementation on industrial control hardware while maintaining high control performance.

5.6. *Sensitivity analysis*

To evaluate the robustness of the proposed MPC–NN–PID controller against model parameter variations, a sensitivity analysis was conducted by simultaneously perturbing the key system parameters a_2 and a_3 within ±20% of their nominal values. These parameters represent the dynamic coupling and response characteristics between the turbine and generator subsystems in the BTG (boiler–turbine–generator) model.

Figure 19 illustrates the three-dimensional surface of the overshoot variation under parameter perturbations. The horizontal axes denote the normalized parameter ratios $a_2/a_{2,nom}$ and $a_3/a_{3,nom}$, while the vertical axis represents the percentage overshoot of the generator output.

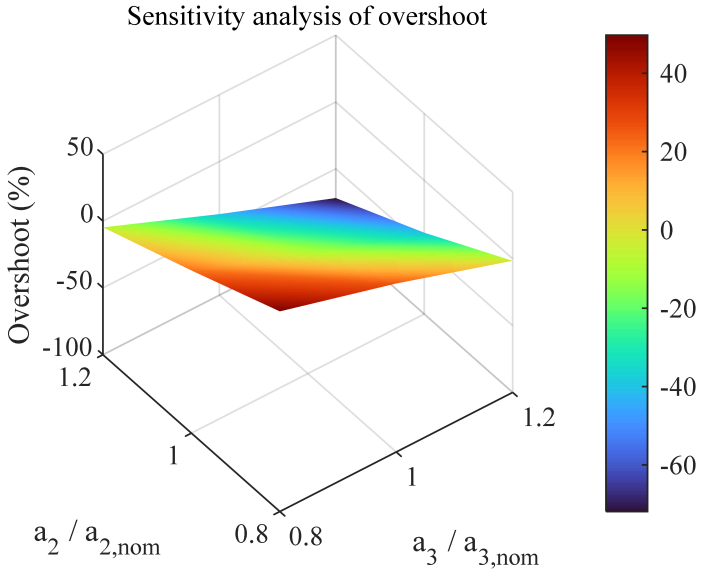

Figure 19. Overshoot sensitivity analysis.

The results indicate that the overshoot remains nearly unchanged within the perturbation range, with only a slight and smooth variation as parameters deviate from their nominal values. This demonstrates that the proposed controller maintains excellent robustness against model uncertainties and parameter drift. The smooth color transition on the surface further confirms the continuity and monotonicity of the system's dynamic response, implying that no abrupt nonlinear instability occurs under moderate parameter deviations.

In summary, the sensitivity analysis verifies that the MPC–NN–PID control structure exhibits high resilience to variations in the BTG system dynamics. Even under ±20% changes in key parameters, the system maintains minimal overshoot and stable convergence, ensuring reliable power control performance under real-world uncertainties such as fuel quality or load fluctuations.

5.7. *Comparative discussion with other advanced control strategies*

Compared with fuzzy PID and adaptive MPC strategies, the proposed MPC–NN–PID controller offers a distinct balance between adaptability and predictive capability. Fuzzy PID controllers rely on rule-based inference for online adjustment but lack long-term predictive planning. Adaptive MPC

methods improve prediction adaptability but involve high computational costs when applied to full-scale nonlinear BTG models. The MPC–NN–PID strategy integrates global predictive optimization with local neural network-based adaptation, achieving faster convergence and higher robustness under actuator constraints. This design ensures that the proposed controller maintains real-time feasibility while achieving superior control precision and robustness in complex nonlinear environments.

Figure 20 compares the power tracking performance of the proposed MPC–NN–PID controller with that of a fuzzy PID controller under the same boiler–turbine–generator (BTG) model and operating conditions. As shown in the figure, both control schemes are able to follow the target power trajectory; however, the MPC–NN–PID controller exhibits a significantly faster dynamic response, smaller overshoot, and smoother steady-state convergence. Specifically, during the transient phase (0–600 s), the fuzzy PID controller suffers from a slower convergence rate and exhibits evident oscillations caused by nonlinear coupling between subsystems. In contrast, the MPC–NN–PID controller utilizes predictive optimization and adaptive neural tuning to anticipate system behavior and generate smoother control actions. As a result, the steady-state error is nearly eliminated, and the transient oscillations are effectively suppressed. These findings demonstrate that the integration of MPC with a neural network-based adaptive PID mechanism greatly enhances control robustness and adaptability compared to traditional fuzzy-tuned PID schemes, particularly under nonlinear and time-varying operating conditions typical of coal-fired power generation systems.

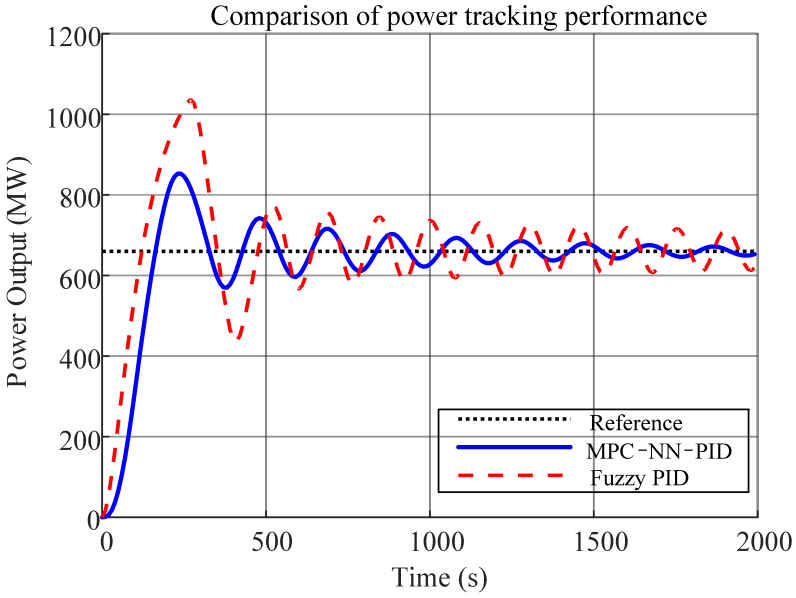

Figure 20. Comparison of power tracking performance between the proposed MPC–NN–PID controller and the fuzzy PID controller.

5.8. Robustness and denoising performance

This subsection investigates the robustness and denoising capability of the proposed MPC–NN–PID framework under measurement noise and model perturbations. To further evaluate the controller's resilience, simulation experiments were conducted by introducing Gaussian noise and

parameter variations into the BTG model. Figure 21 illustrates the robustness and denoising performance of the proposed MPC–NN–PID control strategy under simulated sensor noise and parameter perturbations. To emulate realistic measurement uncertainty, Gaussian noise with a 25 dB signal-to-noise ratio (SNR) was added to the generator power signal, and ±10% parameter perturbations were introduced to the BTG model. The red dashed curve represents the noisy measurement, while the blue curve shows the output after discrete wavelet transform (DWT)-based denoising [59, 60].

The results clearly indicate that the proposed controller maintains stable tracking performance even in the presence of significant disturbances. The noisy signal exhibits rapid oscillations and transient deviations, but after DWT processing, the power trajectory closely aligns with the original (noise-free) output. This demonstrates that the system possesses strong disturbance-rejection capability and that lightweight denoising techniques, such as wavelet-based filtering, can effectively enhance measurement reliability without introducing time delay or overshoot.

Overall, the experiment confirms the robustness and noise immunity of the MPC–NN–PID framework, supporting its applicability for practical implementation in coal-fired power plants where sensor noise and operational fluctuations are unavoidable.

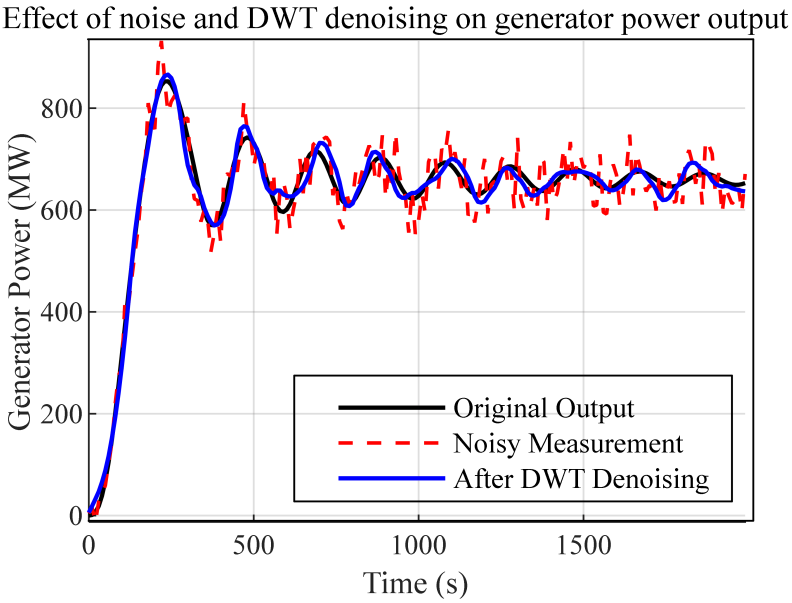

Figure 21. Robustness and denoising performance of the proposed MPC–NN–PID controller under measurement noise and parameter perturbations.

6. Conclusions

This study proposes a hierarchical composite control framework that integrates MPC with a NN–PID controller to enhance the power control performance of coal-fired generator units. By combining the global predictive optimization capability of MPC with the local adaptive learning capability of the NN–PID controller, the proposed method effectively resolves the long-standing contradiction between fast response and system stability in nonlinear thermal systems.

A novel hierarchical control architecture is established, where the upper-layer MPC performs real-time optimal trajectory planning under operational constraints, and the lower-layer NN–PID ensures rapid and robust local tracking. This structure achieves dynamic decoupling between prediction and execution, enabling smooth and overshoot-free power regulation.

Simulation results confirm that the proposed method significantly outperforms both conventional PID and standalone BP–NN–PID controllers. Specifically, the overshoot is reduced from 43.9% to 3.0%, the settling time is shortened to 450 s, and the integral of absolute error (IAE) decreases by 85%. These results demonstrate the effectiveness of predictive optimization in improving both transient and steady-state performance.

The proposed strategy achieves substantial performance enhancement through algorithmic innovation alone, without requiring any hardware modification. It meets the needs of modern coal-fired units for deep peak shaving and fast load-following under high renewable energy penetration, offering a feasible and cost-effective pathway for the intelligent and flexible upgrading of traditional thermal power plants.

Future work will focus on incorporating nonlinear or adaptive MPC frameworks to enhance robustness against time-varying disturbances such as coal quality fluctuations and fuel feed variations. Moreover, the proposed hierarchical concept will be extended to multi-variable coordinated control and hybrid renewable–thermal systems to achieve higher levels of optimization and intelligence in low-carbon energy systems.

Author contributions

Minan Tang: Conceptualization, Data curation, Funding acquisition, Methodology, Project administration, Resources, Supervision, Writing-review & editing. Shengqi Zhang: Conceptualization, Writing - original draft, Software, Formal analysis, Investigation, Validation. Zhongcheng Bai: Conceptualization, Formal analysis, Visualization. Chuntao Rao: Investigation, Validation, Visualization.

Acknowledgments (All sources of funding of the study must be disclosed)

This work was financially supported by the National Natural Science Foundation of China [grant numbers 62363022, 61663021, 71763025, and 61861025]; Natural Science Foundation of Gansu Province [grant number 23JRRA886]; Gansu Provincial Department of Education: Industrial Support Plan Project [grant number 2023CYZC-35].

Use of Generative-AI tools declaration

The authors used ChatGPT (OpenAI) only for minor language refinement. All scientific content, including the model design, algorithms, experiments, data analysis, and conclusions, was created solely by the authors. All AI-assisted text was thoroughly reviewed and edited by the authors.

Conflict of interest

All authors declare no conflicts of interest in this paper.

References

1. Y. B. Shu, G. P. Chen, J. B. He, F. Zhang, Building a new electric power system based on new energy sources, *Eng. Sci.*, **23** (2021), 61–69. https://doi.org/10.15302/J-SSCAE-2021.06.003
2. L. B. Liu, Y. Wang, Z. Wang, S. C. Li, J. T. Li, G. He, et al., Potential contributions of wind and solar power to China's carbon neutrality, *Resour. conserv. recycl.*, **180** (2022), 106155. https://doi.org/10.1016/j.resconrec.2022.106155
3. M. Dreidy, H. Mokhlis, S. Mekhilef, Inertia response and frequency control techniques for renewable energy sources: A review, *Renew. Sust. Energ. Rev.*, **69** (2017), 144–155. https://doi.org/10.1016/j.rser.2016.11.170
4. G. Q. Yu, K. T. Liu, Z. M. Hu, N. N. Liu, X. Y. Xiao, Optimal scheduling of deep peak regulation for thermal power units in power grid with large-scale new energy, *Electr. Power Eng. Technol.*, **42** (2023). https://doi.org/10.12158/j.2096-3203.2023.01.029
5. L. M. Abadie, J. M. Chamorro, Valuing flexibility: the case of an integrated gasification combined cycle power plant, *Energy Econ.*, **30** (2008), 1850–1881. https://doi.org/10.1016/j.eneco.2006.10.004
6. R. A. Mikulandric, D. M. Loncar, D. Cvetinović, Improvement of environmental aspects of thermal power plant operation by advanced control concepts, *Therm. Sci.*, **16** (2012), 759–772. https://doi.org/10.2298/TSCI120510134M
7. X. Hao, C. Yang, H. Chen, J. N. Dong, J. D. Bao, H. Wang, et al., Optimization of the load command for a coal-fired power unit via particle swarm optimization-long short-term memory model, *Energies*, **17** (2024), 2668. https://doi.org/10.3390/en17112668
8. H. Rao, F. Han, Z. Chen, G. Huang, D. Wang, Y. Zhang, et al., Strategy for guaranteeing power supply security of China, *Strateg. Stud. Chin. Acad. Eng.*, **25** (2023), 100–110. https://doi.org/10.15302/j-sscae-2023.02.009
9. D. Wang, H. Li, N. C. Wang, Y. L. Zhou, X. L. Li, M. Yang, Thermodynamic analysis of coal-fired power plant based on the feedwater heater drainage-air preheating system, *Appl. Therm. Eng.*, **185** (2021), 116420. https://doi.org/10.1016/j.applthermaleng.2020.116420
10. W. Wang, Y. Sun, S. Jing, W. Q. Zhang, C. Cui, Improved boiler-turbine coordinated control of CHP units with heat accumulators by introducing heat source regulation, *Energies*, **11** (2018), 2815. https://doi.org/10.3390/en11102815
11. K. J. Åström, T. Hägglund, The future of PID control, *Control Eng. Pract.*, **9** (2001), 1163–1175. https://doi.org/10.1016/S0967-0661(01)00062-4
12. R. Munje, S. Lin, G. Q. Zhang, W. D. Zhang, Observer-based output feedback integral control for coal-fired power plant: A three-time-scale perspective, *IEEE Trans. Control Syst. Technol.*, **28** (2018), 601-608. https://doi.org/10.1109/TCST.2018.2879045

13. A. Boulkroune, M. M'Saad, M. Farza, Adaptive fuzzy controller for multivariable nonlinear state time-varying delay systems subject to input nonlinearities, *Fuzzy Sets Syst.*, **164** (2011), 45–65. https://doi.org/10.1016/j.fss.2010.09.001

14. R. Nasiri , A. Radan, Adaptive decoupled control of 4-leg voltage-source inverters for standalone photovoltaic systems: Adjusting transient state response, *Renewable Energy*, **36** (2011), 2733–2741. https://doi.org/10.1016/j.renene.2011.03.007

15. S. C. Tong, C. Y. Li, Y. M. Li, Fuzzy adaptive observer backstepping control for MIMO nonlinear systems, *Fuzzy Sets Syst.*, **160** (2009), 2755–2775. https://doi.org/10.1016/j.fss.2009.03.008

16. Y. Wang, L. Nie, Application of fuzzy control on smart car servo steering system, *Adv. Sci. Lett.*, **4** (2011), 2099–2103. https://doi.org/10.1166/asl.2011.1471

17. D. Rastovic, Tokamak design as one sustainable system, *Neural Netw. World*, **21** (2011), 493. https://doi.org/10.14311/NNW.2011.21.029

18. M. Chen, C. S. Jiang, Q. X. Wu, Disturbance-observer-based robust flight control for hypersonic vehicles using neural networks, *Adv. Sci. Lett.*, **4** (2011), 1771–1775. https://doi.org/10.1166/asl.2011.1491

19. V. A. Akpan, G. D. Hassapis, Nonlinear model identification and adaptive model predictive control using neural networks, *ISA Trans.*, **50** (2011), 177–194. https://doi.org/10.1016/j.isatra.2010.12.007

20. E. Irigoyen, M. Larrea, J. Valera, V. Gómez, F. Artaza, A hybridized neuro-genetic solution for controlling industrial R3 workspace, *Neural Netw. World*, **20** (2010), 811.

21. J. Garrido, F. Vázquez, F. Morilla, Centralized multivariable control by simplified decoupling, *J. Process Control*, **22** (2012), 1044–1062. https://doi.org/10.1016/j.jprocont.2012.04.008

22. C. Cha, S. Y. Kim, L. Cao, H. Kong, Decoupled control of stiffness and permeability with a cell-encapsulating poly (ethylene glycol) dimethacrylate hydrogel, *Biomaterials*, **31** (2010), 4864–4871. https://doi.org/10.1016/j.biomaterials.2010.02.059

23. I. García-Herreros, X. Kestelyn, J. Gomand, R. Coleman, P. J. Barre, Model-based decoupling control method for dual-drive gantry stages: A case study with experimental validations, *Control Eng. Pract.*, **21** (2013), 298–307. https://doi.org/10.1016/j.conengprac.2012.10.010

24. S. Dettori, V. Iannino, V. Colla, A. Signorini, An adaptive fuzzy logic-based approach to PID control of steam turbines in solar applications, *Appl. Energy*, **227** (2018), 655–664. https://doi.org/10.1016/j.apenergy.2017.08.145

25. Z. Zeng, T. Huang, New passivity analysis of continuous-time recurrent neural networks with multiple discrete delays, *J. Ind. Manag. Optim.*, **7** (2011), 283. https://doi.org/10.3934/jimo.2011.7.283

26. F. Liu, X. Xue, Subgradient-based neural network for nonconvex optimization problems in support vector machines with indefinite kernels, *J. Ind. Manag. Optim.*, **12** (2016), 285–301. https://doi.org/10.3934/jimo.2016.12.285

27. S. A. Elfandi, M. A. Osman, N. Ali, *Application of neural networks and PID in on line of real-time temperature control system,in Appl. Mech. Mater.*, Trans Tech Publications Ltd, **110** (2012), 5009-5014. https://doi.org/10.4028/www.scientific.net/AMM.110–116.5009

28. K. S. Narendra, Identification and control of dynamical systems using neural networks, *IEEE Trans. Neural Netw.*, **1** (1989), 183–192. https://doi.org/10.1109/72.80231

29. X. J. Liu, C. W. Chan, Neuro-fuzzy generalized predictive control of boiler steam temperature, *IEEE Trans. Energy Convers.*, **21** (2006), 900–908. https://doi.org/10.1109/TEC.2005.853758

30. F. Dai, Y. Yan, B. Wei, Y. X. Ouyang, L. R. An, Simulation of main steam temperature control system based on neural network, *J. Robotics Netw. Artif. Life*, **5** (2018), 63–66. https://doi.org/10.2991/jrnal.2018.5.1.14

31. K. Y. Han, G. Y. Park, M. K. Lee, D. H. Yoo, H. H. Lee, Self-adjusting PID control system using a neural network for a binary power plant, *Artif. Life Robot.*, **29** (2024), 274–285. https://doi.org/10.1007/s10015-024-00940-z

32. D. T. Mugweni, H. Harb, Neural networks-based process model and its integration with conventional drum level pid control in a steam boiler plant, *Int. J. Eng. Manuf.*, **11** (2021), 1. https://doi.org/10.12968/S2514-9768(22)90056-0

33. G. Moustafa, F. Noureddinece, A. M. El-Rifaie, A. R. Ginidi, Fractional order PID controller tuned–artificial protozoa optimiser for LFR in multi-area interconnected power systems, *Sci. Afr.*, 2025, e02880. https://doi.org/10.1016/j.sciaf.2025.e02880

34. A. M. El-Rifaie, S. Abid, A. R. Ginidi, A. M. Shaheen, Fractional order PID controller based-neural network algorithm for LFC in multi-area power systems, *Eng. Rep.*, **7** (2025), e70028. https://doi.org/10.1002/eng2.70028

35. S. Abid, A. M. El-Rifaie, M. Elshahed, A. R. Ginidi, A. M. Shaheen, G. Moustafa, et al., Development of slime mold optimizer with application for tuning cascaded PD-PI controller to enhance frequency stability in power systems, *Mathematics*, **11** (2023), 1796. https://doi.org/10.3390/math11081796

36. S. Chandrasekharan, R. C. Panda, B. N. Swaminathan, Modeling, identification, and control of coal-fired thermal power plants, *Rev. Chem. Eng.*, **30** (2014), 217–232. https://doi.org/10.1515/revce-2013-0022

37. D. Wang, X. Wu, J. Shen, An efficient robust predictive control of main steam temperature of coal-fired power plant, *Energies*, **13** (2020), 3775. https://doi.org/10.3390/en13153775

38. X. Liang, Y. Li, X. Wu, Nonlinear modeling and inferential multi-model predictive control of a pulverizing system in a coal-fired power plant based on moving horizon estimation, *Energies*, **11** (2018), 589. https://doi.org/10.3390/en11030589

39. B. Ping, D. Zeng, Y. Hu, Y. Xie, Neural network predictive controller based on the improved TPA–LSTM model for ultra-supercritical units, *Heliyon*, **10** (2024), 12. https://doi.org/10.1016/j.heliyon.2024.e31997

40. G. Shi, M. Ma, D. Li, Y. J. Ding, K. Y. Lee, A process-model-free method for model predictive control via a reference model-based proportional–integral–derivative controller with application to a thermal power plant, *Front. Control Eng.*, **4** (2023), 1185502. https://doi.org/10.3389/fcteg.2023.1185502

41. T. Zhang, S. Gao, Y. Yang, S. X. Wang, Z. Ding, Economic model predictive control of thermal-power boiler–turbine units with extreme learning machine–deep belief network, *Eng. Appl. Artif. Intell.*, **162** (2025), 112505. https://doi.org/10.1016/j.engappai.2025.112505

42. D. Q. Mayne, J. B. Rawlings, C. V. Rao, P. O. M. Scokaert, Constrained model predictive control: Stability and optimality, *Automatica*, **36** (2000), 789–814. https://doi.org/10.1016/S0005-1098(99)00214-9

43. X. Liu, J. Cui, Economic model predictive control of boiler-turbine system, *J. Process Control*, **66** (2018), 59–67. https://doi.org/10.1016/j.jprocont.2018.02.010

44. L. Gao, Y. Yang, X. Ren, Temperature MPC strategy for air source heat pump based on BP neural network, *Control Eng.*, **28** (2021), 1765–1772.

45. X. Kong, X. Liu, K. Y. Lee, Nonlinear multivariable hierarchical model predictive control for boiler-turbine system, *Energy*, **93** (2015), 309–322. https://doi.org/10.1016/j.energy.2015.09.030

46. S. Liu, B. Zhao, S. Zhao, L. Y. Zhang, L. Wu, An intelligent bio-inspired cooperative decoupling control strategy for the marine boiler-turbine system with a novel energy dynamic model, *Energies*, **12** (2019), 4659. https://doi.org/10.3390/en12244659

47. P. Appeltans, S. I. Niculescu, W. Michiels, Analysis and design of strongly stabilizing PID controllers for time-delay systems, *SIAM J. Control Optim.*, **60** (2022), 124–146. https://doi.org/10.1137/20M136726X

48. J. Kang, W. Meng, A. Abraham, H. B. Liu, An adaptive PID neural network for complex nonlinear system control, *Neurocomputing*, **135** (2014), 79–85. https://doi.org/10.1016/j.neucom.2013.03.065

49. E. Hernandez, Y. Arkun, Study of the control-relevant properties of backpropagation neural network models of nonlinear dynamical systems, *Comput. Chem. Eng.*, **16** (1992), 227–240. https://doi.org/10.1016/0098-1354(92)80044-A

50. S. J. Qin, T. A. Badgwell, A survey of industrial model predictive control technology, *Control Eng. Pract.*, **11** (2003), 733–764. https://doi.org/10.1016/S0967-0661(02)00186-7

51. E. Fernandez-Camacho, C. Bordons-Alba, *Model predictive control in the process industry*, Springer London, 1995.

52. X. Y. Huang, J. C. Wang, L. W. Zhang, B. H. Wang, Data-driven modelling and fuzzy multiple-model predictive control of oxygen content in coal-fired power plant, *Trans. Inst. Meas. Control*, **39** (2017), 1631–1642. https://doi.org/10.1177/0142331216644498

53. A. S. Kumar, Z. Ahmad, Model predictive control (MPC) and its current issues in chemical engineering, *Chem. Eng. Commun.*, **199** (2012), 472–511. https://doi.org/10.1080/00986445.2011.592446

54. S. Agbleze, L. J. Shadle, F. V. Lima, Dynamic modeling and simulation of a subcritical coal-fired power plant under load-following conditions, *Ind. Eng. Chem. Res.*, **63** (2024), 11044–11056. https://doi.org/10.1021/acs.iecr.4c00494

55. C. Maffezzoni, Issues in modelling and simulation of power plants, *IFAC Proc. Vol.*, **25** (1992), 15–23. https://doi.org/10.1016/S1474-6670(17)50423-1

56. J. W. Jang, J. J. L. Velázquez, On the temperature distribution of a body heated by radiation, *SIAM J. Math. Anal.*, **56** (2024), 3478–3508. https://doi.org/10.1137/23M1580917

57. A. Lawal, M. Wang, P. Stephenson, O. Obi, Demonstrating full-scale post-combustion CO_2 capture for coal-fired power plants through dynamic modelling and simulation, *Fuel*, **101** (2012), 115–128. https://doi.org/10.1016/j.fuel.2010.10.056

58. J. A. Carrillo, J. Mateu, M. G. Mora, L. Rondi, L. Scardia, J. Verdera, The ellipse law: Kirchhoff meets dislocations, *Commun. Math. Phys.*, **373** (2020), 507–524. https://doi.org/10.1007/s00220-019-03368-w

59. M. Z. Yousaf, A. R. Singh, S. Khalid, M. Bajaj, B. H. Kumar, I. Zaitsev, Bayesian-optimized LSTM–DWT approach for reliable fault detection in MMC-based HVDC systems, *Sci. Rep.*, **14** (2024), 17968. https://doi.org/10.1038/s41598-024-68985-5

60. M. Z. Yousaf, A. R. Singh, S. Khalid, M. Bajaj, B. H. Kumaret, I. Zaitsev, Enhancing HVDC transmission line fault detection using disjoint bagging and Bayesian optimization with artificial neural networks and scientometric insights, *Sci. Rep.*, **14** (2024), 23610. https://doi.org/10.1038/s41598-024-74300-z

AIMS Press